ENGINEERING HYDROGEL ENVIRONMENTS TO DIRECT CELL FATE

BY

SAMUEL H MO

THESIS

Submitted in partial fulfillment of the requirements
for the degree of Master of Science in Materials Science and Engineering
in the Graduate College of the
University of Illinois at Urbana-Champaign, 2016

Urbana, Illinois

Adviser:

Professor Kristopher Kilian

Abstract

The advent of hydrogels for biological applications has sparked interest in the both the medical and engineering community in recent years as a means to investigate cellular level processes. An area that has shown promising application of hydrogel materials has been in the study of stem cell development. Proven that the microenvironment of the stem cell plays a critical role in its development, hydrogels can closely mimic the intricate physical, biological, and chemical landscape encompassing various cell types. Hydrogels are simply polymer network with large water content, and their robust nature allows versatile manipulation. From patterning different geometries, coating with adhering proteins or bioactive peptides, and construction of complex physiological architectures, hydrogels provide a wide set of tools to investigate stem cell development. Interested in a wide range of questions in cellular development, we explored effects of different aspects of the environment. We patterned polyacrylamide hydrogels with patterns similar topologically to tissue architecture to observe increased conversion, used this system with it's tunable compliance to study natural biochemical lipid derivatives to observe significant cellular response, and created PEG based 3D coculture environments to study the interface of cell types for increased angiogenesis.

Acknowledgements

I would like to express my gratitude and thankfulness to my principal investigator Professor Kristopher Kilian and the Kilian lab to engage in exciting phenomena found in stem cell biology and engineer biomaterials to explore the vast unknown. My time at the Kilian lab has been a humbling experience providing a glimpse of the true complexity of nature while showcasing the large hurdles involved with engineering novel materials to investigate these biological questions. Starting as a naïve undergraduate with large expectations and big dreams, I was graciously given the freedom to explore many individual projects that did not reach full maturity. My first big interest which made me gravitate towards the Kilian lab was the mystery surrounding the lack of regeneration in cardiac tissue, specifically in cardiomyocytes. Curious to explore if the combinatorial effect of electrophysiological and physical cues can optimize cardiac lineage specification, I attempted to create an electroconductive hydrogel system with architecture to encourage cardiomyogenesis. Another project that captured my interest was exploring the temporal mechanical remodeling cells exerted during direct reprogramming. As a phenomena only discovered recently, the morphogenesis and physical response of somatic cells during reprogramming can provide insight into developing materials that can optimize the process with future implications in regenerative medicine. Although the platform of hydrazone hydrogels was ready, we ran into difficulty with the biology of transfecting the necessary factors to directly reprogram MEFs into cardiomyocytes. Lastly, I was interested in developing hypoxic hydrogels that would provide an assay to study many biological questions in ischemic tissue or hypoxic environments such as cancer stem cells. Without a fuller background in synthetic chemistry, this project proved more time consuming than allotted for during the masters. Overall, the generous freedom to explore many of these projects that did not reach full maturity assured my conviction for science and engineering, but it also taught me the valuable lesson of scientific realism, with intentional and meticulous purpose for the greater good of society. I would like to thank Professor Kristopher Kilian for all his support and Amr Abdeen specifically for his thoughtful, thorough, and caring mentorship.

Table of Contents

List of Abbreviations

AEA – Arachidonoyl Ethanolamide
AKT – (AK) designates strain of mice found to yield high number of spontaneous thymic lymphomas, and (T) describes the transforming retrovirus isolated. Human homologues of Akt are oncogenes found to regulate normal cell function
Ald –Aldehyde
APS - Ammonium persulfate
APTS - (3 – aminopropyl)triethoxysilane
B3 Tub – Beta III tubulin
CYP – Cytochrome P450
DHEA – Dehydroepiandrosterone
DI – Deionized water
DMSO - Dimethylsulfoxide
ECM – Extracellular Matrix
EDP – Epoxydocosapentaenoic Acid
EEQ – Epoxyeicosatetraenoic Acid
EET – Epoxyeicosatrienoic Acid
EPA – Eicosapentaenoic acid
EtOH – Ethanol
FA – Focal adhesion
GPCR – G-protein coupled receptor
Hz – Hydrazine
LCPUFA – Long chain polyunsaturated fatty acid
MAP2 – Microtubule associated protein 2
MSC – Mesenchymal stem cell
PA – Polyacrylamide
PEG – Polyethylene glycol
PPARg – Peroxisome proliferator-activated receptor
SB – Sodium butyrate
TEMED – Tetramethylethylenediamine
VPA – Valporic acid

Chapter 1

Hydrogels for Cell Culture

1.1 Beginnings of hydrogels in Cell Study

1.1.1 – *Historical origin of hydrogel*

The coined term hydrogel has existed since 1894 for a colloidal gel of inorganic salts, but the first time the commonly accepted definition of a hydrogel was seen in literature occurred in 1960 by Wichterle and Lim[1]. In the 1960's, poly (hydroxyethylmethacrylate) (pHEMA) was developed exhibiting the high affinity for water properties well accepted in the modern community and it was originally developed for uses in human tissue[2]. Since then, hydrogel science has been observed to develop in three stages from the first generation developing gels with high swelling, to the second generation incorporating external stimuli, and the current generation investigating complex material interactions[1].

1.1.2 – *Modern definition of hydrogel*

A general understanding of a hydrogel is a matrix of polymers that swell, but don't dissolve in water, at least for the short term[3]. Swelling within a hydrogel can be explained by high thermodynamic affinity of the matric for the solvent itself, establishing equilibrium with the solvent given its temperature, to develop the shape and mechanical properties of the swollen gel. Different variations in the polymers from concentration, structure, cross-linker and mixtures can lead to different properties and shapes within hydrogels. As imaginable, a multitude of gel systems have been engineered and discovered for a wide variety of applications in engineering and science, even in stem cell science.

1.1.3 – *Common types of hydrogels*

In the past decade, the exponential interest in hydrogel materials have accelerated modifications in hydrogels such as hydrogel systems with responsive moieties that respond to external stimuli such as temperature, ionic concentration, UV exposure, pH, magnetic fields, and other chemicals[4–6]. Furthermore, matrices have been developed to incorporate two or more of these response moieties for specific functions[7]. These smart hydrogel systems change structural and volumes in response to these stimuli allowing a wide variety of applications for scientific observations[8].

Over the past decades, many polymers have been utilized to create hydrogel systems, and they span a wide range of materials that can be classified as either natural or synthetic. Natural hydrogel systems incorporate derivatives of materials found in nature such as collagen, hyaluronic acid, fibrin, alginate, chitosan, Matrigel, and more[9,10,11,12,13]. Natural hydrogels generally outperform synthetic materials as they mimic components of the natural extracellular matrix (ECM). Although natural hydrogels are advantageous in this way, their preset chemical structures make it difficult to control the final hydrogel microstructure and reproduce microstructures between experiments. Furthermore, the components from natural hydrogels must be extracted from animal or plant sources making it difficult to control the composition of the starting materials[9–13]. Opposed to extracting monomers from natural origins, synthetic hydrogels such as poly (acryl-amide) (PA), poly (ethylene glycol) (PEG), and poly (vinyl alcohol) (PVA), are reproducible and their final structure can be controlled through the gelation protocol and environment[14–16]. Synthetic hydrogels can be chemically modified to have smart properties such as hydro-lysability to external stimuli and natural degradation[17,18].

1.1.4 – *Physical vs Chemical hydrogels*

Hydrogels can also be understood molecularly as either a reversible/physical gel or a permanent/chemical gel[19]. Physical gels are hydrogels that use entanglement or secondary forces such

as H-bonds, hydrophobic forces, London dispersion forces, and ionic forces to hold its structure and these physical gels are usually not homogenous as pockets of entanglement. Chemical gels on the other hand are networks where polymers are covalently linked with another and usually show higher degrees of homogeneity if not mainly homogenous.

1.2 Hydrogel Characterization

1.2.1 – *Hydrogel Crosslinking*

Crosslinking is a major component of hydrogel structure which can be correlated to every characteristic of a hydrogel[7]. Crosslinking within a hydrogel can vary widely, but can be explained through physical or chemical interactions. Methods for crosslinking include UV radical polymerization, heating, or chemical reactions[5]. Due to the wide variety of crosslinking methods, the same starting polymers can be optimized for many applications by manipulating the properties of the formed hydrogel.

1.2.2 – *Hydrogel Swelling*

Hydrogels primary characteristic is its ability to swell to allow free diffusion of solute molecules[20]. The polymer matrix holds water absorbing a fraction of their dry weight in liquid up to several thousand times[3]. The percentage of water held in a hydrogel can determine permeation of cellular materials through the gel such as nutrients, ions, cellular waste and debris. After polymerization of the hydrogel, placement into water will swell the hydrogel where the first water molecules entering the gel will hydrate the most polar, hydrophilic groups. As the water intercalates through the gel hydrating the most polar, hydrophilic groups the network will start to swell and exposes hydrophobic groups. Water molecules will interact with the hydrophobic groups leading to secondary bound water molecules. After initial swelling, the network will swell further due to osmotic driving forces for dilution of the network chains until it is opposed by the crosslinked polymer network meeting an elastic network

retraction force. Free water will fill any remaining space between chains, in pores, and voids after all interacting groups with water have saturated. If the network chains are degradable, then the hydrogel will start to disintegrate and dissolve at a rate dependent on the concentration of the degradable moiety as the gel swells[21].

Not only can swelling be controlled, but so can the mechanical properties of the gel be tuned by varying the cross-linking degree with changes in composition or structure. Changing the mechanical properties can serve many purposes based on the aim a particular study. A wide list of variables can be responsible for changes in mechanical properties and different analysis techniques are appropriate to explain different causes. These properties include the Young's modulus, Poisson's ratio, storage and loss moduli which can be measured by AFM, rheology, DMA, and many more techniques.

1.2.3 – *Hydrogel Porosity*

Pores form in hydrogels through phase separation during synthesis[21]. The size of the pore, distribution of pore sizes, and pore interconnectivity are important mechanical factors in the matrix that prove to be difficult to quantify[22]. One method to estimate pore sizes utilizes labeled probes of varying molecular weights and sizes. When considering hydrogels porosity, it is primarily affected by three factors. First, pore size can be attributed to the concentration of chemical cross-links which is defined by the ratio of the cross-linker to the monomer. Secondly, pore size distribution can be attributed to the concentration of physical entanglements of polymer chains defined by polymerizable monomers in solution. Lastly, the net charge of the hydrogel can affect pore size distribution defined by the concentration of cationic or anionic monomers[23]. Apart from the concentration of cross linkers, monomers, and ionic species, the surrounding solution dissolved charged and uncharged solutes will distribute unevenly between gel and solution phase and will affect pore size distribution.

1.3 Applications of hydrogels in science and technology

The rise of hydrogel materials the past decade has increased the occurrence and observance of their applications in many fields[21]. In the field of medicine, hydrogels have been popular in the usage of lens materials for ocular devices and research[24]. Another notable application of hydrogels in the field of medicine can be seen in surgery[17]. As good materials for physiological compatibility for ECM like properties, hydrogels have been attempted for use as new materials for body reconstruction. For example, Hyaluronic acid has been applied in tissue filling applications[25]. Hydrogels have also been used as bulking agents for urinary incontinence where the material can constrict the urethra to reduce patient's incontinence[26]. Even beyond medical purposes, hydrogels have trickled into the world of plastic surgery with breast size enhancements as an alternative to silicon prosthetics.

1.3.1 – *Clinical applications*

The wide range of clinical uses of hydrogels show the versatility of its applications, but they can be further seen in the rising field of immunotherapy and vaccine design[13]. Nanofibrous hydrogels have proven to condense bioactive DNA that lead to immune response to HIV which circumvents the risks of using live or attenuated viruses to fight HIV infection[27]. These DNA vaccines can be degraded by natural DNases and lysosomes later. The advantages of using hydrogels for immunotherapy include its high loading capacity, safe working conditions, and acceptable biocompatibility[28].

1.3.2 – *Tissue engineering*

Engineering advances of hydrogel materials have led to their application in the field of tissue engineering where hydrogels can serve as 3D scaffolds. They provide promising uses for in-vivo tissue

regeneration where autologous cells are encapsulated into the polymer, and cultured until ready for implantation. The strategy of scaffolds seek to promote cell proliferation and tissue re-growth by mimicking the ECM as physiologically as possible. This would require incorporation of growth factors, metabolites, biological cues, topographical architecture, etc. to promote natural tissue healing. These hydrogels may be designed to contain pores that can accommodate living cells that may need to proliferate into the tissue which may require networks that dissolve and degrade over time. Although scaffolds offer promising future therapies, there are limiting factors such as low mechanical strength posing great challenges in handling and incorporation. Furthermore, introduction of any synthetic material poses issues of sterilization and biocompatibility which could impede translation.

1.4 Hydrogels as tools to investigate biological processes

1.4.1 – *Hallmark use to introduce mechanical cues*

In 2006, Engler et al. demonstrated the importance of substrate elasticity in the lineage specification of mesenchymal stem cells (MSCs)[29]. On collagen coated hydrogels, MSCs are cultured on gels of different substrate elasticities and show different morphologies suggesting lineage specification may be directed by the matrix stiffness. The cellular machinery directing the sensing of the substrate stiffness is played largely by focal adhesion complexes where non-muscle myosin II, a crucial protein that contributes to intracellular tension along stress fibers, shows dependence with the response to changes in substrate elasticity. Substrate elasticities of ~0.1 – 1kPa demonstrated neurogenic markers, 8 – 17kPa myogenic markers, and 25 – 40kPa demonstrated osteogenic. An RNA profile also indicated that the MSCs on differing substrate elasticities committed to the lineages mentioned above. As a hallmark experiment demonstrating the importance of mechanotransductive cues in development of

MSCs, the use of hydrogels have since exploded for investigations exploring mechanical influences on biological processes, specifically in early cell development.

1.4.2 – *Elucidating mechanotransduction pathways*

Since the original study from Engler et al., there have been many scientific debates on the holistic nature of mechanical cues on lineage specification, especially regarding the effect of substrate elasticity alone as a sufficient driving force for developmental influence. Arguments have risen challenging the study as incomplete since it failed to recapture the full complexity of physiological microenvironments[30]. Where the study was completed on a 2D surface, other investigators introduced models encapsulating cells in 3D environments with controlled stiffness[31].

Other scientists that oppose the claim that substrate elasticity is a sufficient cue suggest that factors such as tethering density is the true driving force for mechanical sensing within cells[32]. Trappmann et al. demonstrate that on PDMS substrates of different substrate stiffnesses, no different lineage specification is observed compared to the Engler study that seeded cells on PA gels that had varying pore sizes based on the stiffness. Changing the stiffness of PDMS did not exert an influence on lineage specification; however, changing the density of tethered proteins analogous to proteins at the perimeter of different pores on the PDMS substrates showed lineage specification with higher density favoring osteogenic fates and lower density favoring adipogenic fates. More recently, work from the Engler lab demonstrated that stiffness is a critical driver underlying differentiation and that the nature of tethering cannot explain the observed role of stiffness[33].

As many investigators utilize 2D platforms to study mechanobiology, consideration for the differences in dimensionality is important to address as Baker et al. review features that differ in 3D culture systems that influence behavior[34]. In 3D environments, one of the most pronounced

differences is morphology where cells spread on surfaces have forced apical-basal polarity, but cells in 3D morphology retain a stellate morphology[35]. Furthermore, others demonstrate that the degradability of the 3D microenvironment is another important driving force for stem cells to read their environment and respond developmentally[18].

Regardless of which mechanical cue may be the primary driving force within cells, or if these mechanical cues change in priority temporally during cellular development, it is undeniably agreed within the scientific community for developmental biology that mechanotransduction plays a crucial role for stem cell development and lineage specification.

1.5 Hydrogels as model systems

For this work, we used two main model systems to explore hydrogels for stem cell applicatoins: Polyacrylamide and PEG for 2-D and 3-D cell culture, respectively. The rest of this work is dedicated to exploring the use of these two systems in various cell culture applications. In chapter 2, we develop micropatterned PA hydrogels as a model system with tunable mechanical properties with the ability to control cell morphology. We utilize this system in chapter 3 to study the effects of lipid mediators on MSC differentiation. With the aforementioned importance of encapsulating and studying cells in 3-D systems, we introduce PEGDA hydrogels in chapter 4 as a cell-safe system to study cells and their interactions in a 3-D system, using angiogenesis as a model system. Finally, in chapter 5, we attempt to modify a PEG system to introduce malleability to cellular remodeling.

1.5.1 – *Synthesizing polyacrylamide*

To synthesize hydrogels with polyacrylamide for robust patterning, acrylamide, bis-acrylamide (N,N'-methylenebisacrylamide), ammonium persulfate, TEMED (N,N,N',N'-tetramethylethylenediamine) are reacted together. Before polymerizing the acrylate groups from acrylamide and bis, the

stoichiometric mixture of acrylamide and bis is crucial to the extent of crosslinking that leads to varying stiffnesses of synthesized polyacrylamide hydrogel[36].

1.5.2 – *Synthesizing PEG hydrogels*

To create hydrogels with PEG that are robust with many of our applications, the hydroxyl moiety was functionalized with acrylate groups to create PEG diacrylate or PEGDA[37]. PEG of different lengths dependent on the desired substrate elasticity, was dried from atmospheric hydration by co-distillation with toluene at least three times in a rotary evaporator. The residue was then dissolved in dichloromethane and toluene under nitrogen. Wrapping the reaction flask in aluminum foil, all following reactions were protected from light. In the reaction flask, a stir bar was added to stir at medium stirring, then trimethylamine was added followed by addition of acryloyl chloride. This reaction was left overnight at room temperature. This reaction mixture was filtered through a column of aluminum. The remaining acid in the mixture was quenched with addition of K_2CO_3 by stirring in for 1.5 hours. The solid was then removed from the mixture, and placed under vacuum to remove dichloromethane. This product was then precipitated using diethylether under vigorous stirring. After 2 hours, the precipitate was collected by filtering over a glass filter, washed again with diethylether to remove any remaining particle, and then lyophilized. The remaining dried PEGDA was then analyzed using NMR to validate end group modification with acrylate groups.

Chapter 2

Development of Patterned Polyacrylamide Hydrogels as 2-D Culture Model

In this chapter, we seek to extend the utility of PA hydrogels as model systems through the addition of micropatterning functionality in addition to tunable mechanical properties.

2.1 Purpose of patterning hydrogels

2.1.1 – *Mechanotransduction*

The past two decades of research into the influence of mechanical and structural cues on cell behavior has shown increasing evidence of an influence on epigenetic factors that have an important role in cell physiology, development, and disease[38]. The mechanobiology field has been widely driven by a desire to relate mechanotransduction pathways to the biological response where many bioactive molecules are altered in different forms[39]. Individual peptide domains within cytoskeletal proteins undergo stepwise unfolding when mechanically extended which depends on where the load is applied. Since physical loads can affect protein conformation, it will also affect the kinetics of protein-protein or protein-ligand interaction within cells and may often expose cryptic binging sites.

The force generated by myosin on actin filaments extends the lifetime of a bound crosslink, but when the force is dissipated, it disassembles rapidly[40]. Binding kinetics of adhesion receptor complexes found on the cell surface modulate cell adhesion and movement based on adhesion molecule concentration, rate, and force application. Forces on a cell can influence molecular polymerization as well, which is shown in microtubule polymerization when tension on cells is increased by applying forces on ECM adhesions[41].

2.1.2 – *Hierarchy of Mechanotransduction*

Nature has developed a hierarchy of mechanotransduction within cells to convert mechanical cues to biological responses. On a macroscale, pre-stress is generated between tissues and organs to resist and generate force. Zooming in, the forces are distributed among adjacent tissues through cell adhesion to ECM[42]. On a cellular scale, specific mechanotransduction receptors such as integrins couple the cytoskeleton to the ECM and will allow cells to sense the orientation and rigidity of their environment. Integrins connect with the cytoskeleton through focal adhesion complexes that include many actin associated proteins such as vinculin, talin, and paxillin[43]. The force from the ECM is transferred through the integrin which then rearrange actin filaments, microtubules, and intermediate filaments which strengthens the entirety of the cell to protect against any possibility of physical distortion[44]. The force from the ECM onto the cell surface is directed to transmembrane adhesion receptors which are concentrated at focal adhesions that form strong cytoskeletal connections; whereas weak cytoskeletal connections dissipate[45]. The distance from the receptor to the nucleus requires long distance force transfer over the cytoskeleton which is transmitted outwardly to provide structural response to the ECM and can lead expression change in tubulin[46]. Furthermore, the cytoskeletons of cells are prestressed by contracticle microfilaments that are mediated from microtubules and adhesions to the ECM. This relationship differs dependent on cell shapes where in rounded cells the microtubules will experience most of the prestress and spread cells will have most of the force distributed to the anchoring points on adhesive complexes[47]. The mechanical interactions between microtubules, microfilaments, and adhesion complexes modulate the shape and stiffness of cells to their linked ECM. Focusing in on the specific membrane processes such as the filopodia, stereocilia, cilia and flagella, they are also stabilized through the compressive forces onto the cells and the resisting stiffened microfilaments. From the ECM, forces are eventually transferred to the nuclear membrane where the

cortical cytoskeleton balances the force and prevents distortion. A network of actin protofilaments, held by spectrin molecules, in conjunction with nuclear lamins form a geodesic network to resist microtubule compression and tensed chromosomes to stabilize the mitotic spindle[48].

2.1.3 – *Types of Patterning Methods*

There exists many methods to pattern hydrogel systems with desired topographies and geometries. Such techniques include inkjet patterning, embossing, microfluidics, self-assembled monolayer replacements, and photolithography[49]. To highlight a few of the versatile techniques to pattern surfaces, microfluidics and photolithography provide a robust means to specify regions of different adhering layers and print unique geometries. For example, configuring arrays of microfluidic channels can assemble alternating rows of peptides to polarize cells cultured atop the surface[50]. Whereas specifying geometry may prove challenging for flowing channels, microcontact printing can specify multicellular islands or even shapes for single cells attachment[51].

2.1.4 – *Effect of patterning on stem cell fate*

In a classic study by McBeath et al., they demonstrate that MSCs that underwent increased cytoskeletal tension through spread adherence and flattening underwent osteogenesis whereas unspread, rounded MSCs underwent adipogenesis. They highlighted the action of RhoA that regulated the commitment of MSCs where constitutively active expression led to osteogenic fate and negative expression led to adipogenesis[52]. To exemplify this phenomena, Kilian et al. demonstrate that cell geometry itself has a vital role in directing lineage commitment. Using microcontact printing to pattern shapes that would exemplify interfactial strains invoking different levels of cytoskeletal contractility, they demonstrate that on a single cell basis, shapes that experience high levels of actomyosin contractility promote osteogenesis while reduced contractility cells expressed higher percentages of adipose commitment. The concomitant physical cues that translate to different cytoskeletal architectures by patterning cells

in different geometries lead to mechanotransduction on stem or progenitor cells that direct their fate highlighting the importance of investigating the role of geometry itself[51].

The physical microenvironment can drive stem cells to different lineages based on the different interstitial strains and graded stresses that are exerted on patterned geometries confining cells to specific areas. Ruiz et al. demonstrate that groups of mesenchymal stem cells seeded on large circular patterns showed osteogenic lineage specification towards the edge whereas the MSCs toward the center of the multicellular islands prefer an adipogenic lineage. When they measured traction forces generated through the multicellular islands, they observed a gradient of stress that paralleled the preferential differentiation of MSCs where high stress correlated to osteogenic differentiation and low stress correlated to adipogenic differentiation[39].

2.1.5 – *Surface presentation direct response of integrin expression and cell behavior*

The microenvironment comprises of many components from the diverse biochemical interactions composing of paracrine and cytokine network, but is also comprised of many complex physical moieties interacting in concert to drive function and regulation. Discussed in the section above is the importance of the geometric interfaces that drive stem cell behavior, but another factor to consider is the role of the diverse body of adhering moieties that allow cells to contract and translate the mechanical environment. Desai et al. demonstrated that the pallet of integrins specifically interact with different extracelluar matrix proteins which drive cells to migrate across multicomponent surfaces[53]. Majumdar et al. also demonstrate that the surface presentation of different ECM proteins and adhesion complexes will express different integrins in human MSCs using flow cytometry. They demonstrate that specific expression of integrins mirror specific behavior where upregulated ICAM1 expression from IL-1a, TNFa, and IFNg led to preferential interaction with hematopoietic lineages[54]. Wozniak et al. also demonstrate that cells modify focal adhesion complexes based on the composition

of the ECM composition. The focal adhesions are not only regulators that control complex cellular responses to the dimensionality of the environment, but also regulators that response to the diverse body of attaching proteins[55]. Kilian et al. demonstrate that ligand affinity influences integrin adhesion which was tuned to promote osteogenesis, myogenesis, and neurogenesis. Using SAMs to immobilize linear or cyclic RGD, where cyclic RGD had double the affinity for α5β3, an integrin known to promote osteogenesis, expression for Runx2 (osteogenesis) was pronounced on cyclic RGD while expression for MyoD1 (myogenesis) and B3 tubulin (neurogenesis) was increased for linear RGD[56].

2.2 Materials and methods

2.2.1 – *Preparing glass coverslips and microscope glass slides*

The complexit influence of the physical microenvironment on cellular behavior can be studied by patterning hydrogels with microprinting techniques. Using polyarcylamide hydrogels synthesized on chemically treated coverslips provides a robust platform to pattern different geometries and matrix protein presentations to study stem cell behavior. Glass coverslips of 18mm diameter are first cleaned by sonicating in ethanol for fifteen minutes followed by sonication in DI water for another fifteen minutes. These clean glass coverslips are then placed into wells of 12 well plates using a forcep. The wells are then pipetted with 1mL of 0.5 % v/v (3 – aminopropyl)triethoxysilane (APTS) in DI water for three minutes to introduce amine groups on the coverslips (Figure 2.1). The APTS is then aspirated and the coverslips are rinsed three times with DI water. Failure to rinse off residual APTS will result in future delamination of the polyacrylamide gel since the glutaraldehyde will react with free floating APTS and fail to chemically modify free aldehydes on the coverslip.

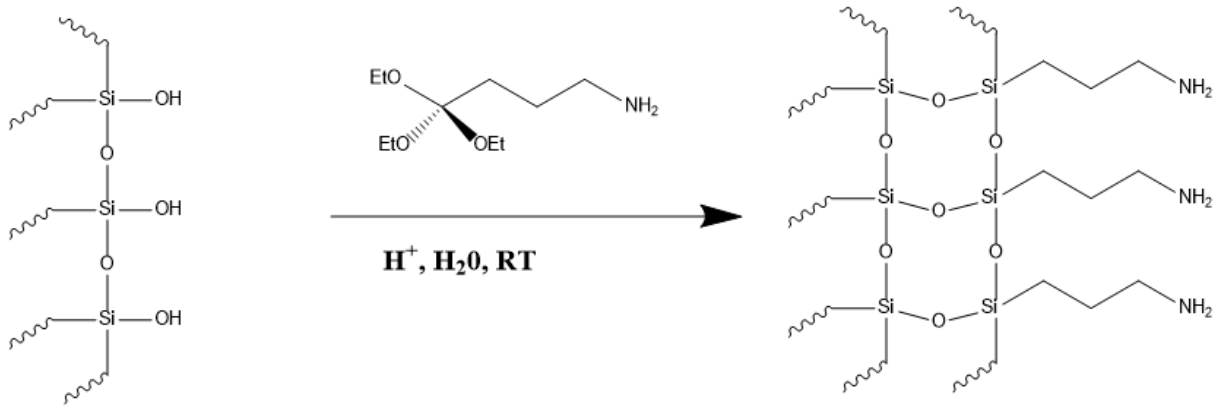

Figure 2. 1 – Treating glass coverslips with APTS introduces amines on the surface for further modification.

After the coverslips are functionalized with APTS to present amine groups, then 1ml of 0.5% v/v glutaraldehyde in DI water is pipetted into each well for thirty minutes to introduce aldehydes on the surface of the coverslip (Figure 2.2).

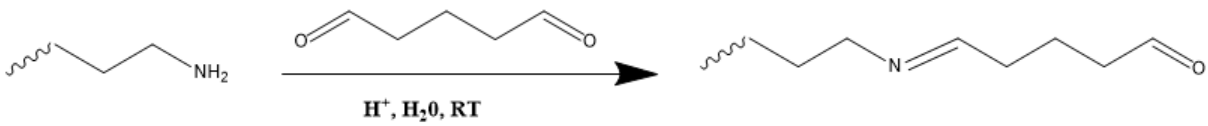

Figure 2. 2 – Sequential treatment of APTS treated coverslips with glutaraldehyde introduces aldehyde groups through acid catalyzed imine formation where protonated carbonyl oxygen favors nucleophilic attack from the amine with dehydration of the protonated oxygen.

Synthesis of polyacrylamide can be initiated by a "hybrid cage-complex" mechanism that occurs between acrylamide and persulfate anion. The monomer-initiator complex leads to a donor-acceptor relationship between the amide and persulfate where the decomposition of this charge-transfer prefers the formation of a peroxide[57]. In a radical mediated fashion, the radicalized acryl groups are now able to polymerize with the acryl groups on acrylamide and bis-acrylamide and this reaction is catalyzed by using tetramethylethylenediamine (TEMED). By varying the composition of acrylamide and bis-acrylamide, the stiffness of polyacrylamide can be altered[36].

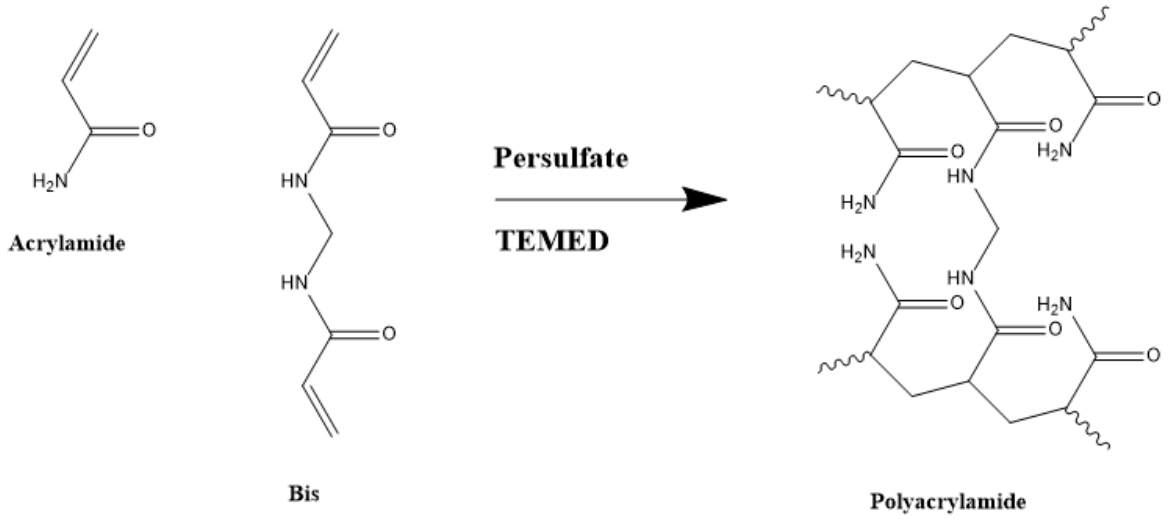

Figure 2. 3 – Formation of polyacrylamide using persulfate anion and TEMED catalyst using radical polymerization using acrylamide and bis.

2.2.2 – *Gelating hydrogels on coverslips*

Polyarcylamide hydrogels are formed on microscope glass slides that are treated with hydrophobic treating agent Rain-X ©. Microscope glass slides are sprayed with Rain-X to chemically alter the silane surface. Sequential use of the microscope glass slides are first cleaned with ethanol, then water, and then resprayed with Rain-X. They are then rinsed with water before a solution of polyacrylamide mixture is pipetted on them. To form polyacrylamide gels on treated coverslips, first the appropriate mixture of acrylamide and bis is prepared and degassed of oxygen using argon for 10 minutes. An appropriate amount of polyarcylamide mixture with initiator and catalyst was prepared in a microcentrifuge tube with 0.1% ammonium persulfate (APS) and 0.1% of TEMED. When the APS and TEMED was pipetted, it was quickly vortexed for about ten seconds, then pipetted 20uL of gel mixture on the hydrophobic glass slide, and then carefully placed the functionalized coverslip on top of the droplets with forceps to form polyacrylamide gels sandwiched between the glass coverslip and micrscope slide (Figure 2.4).

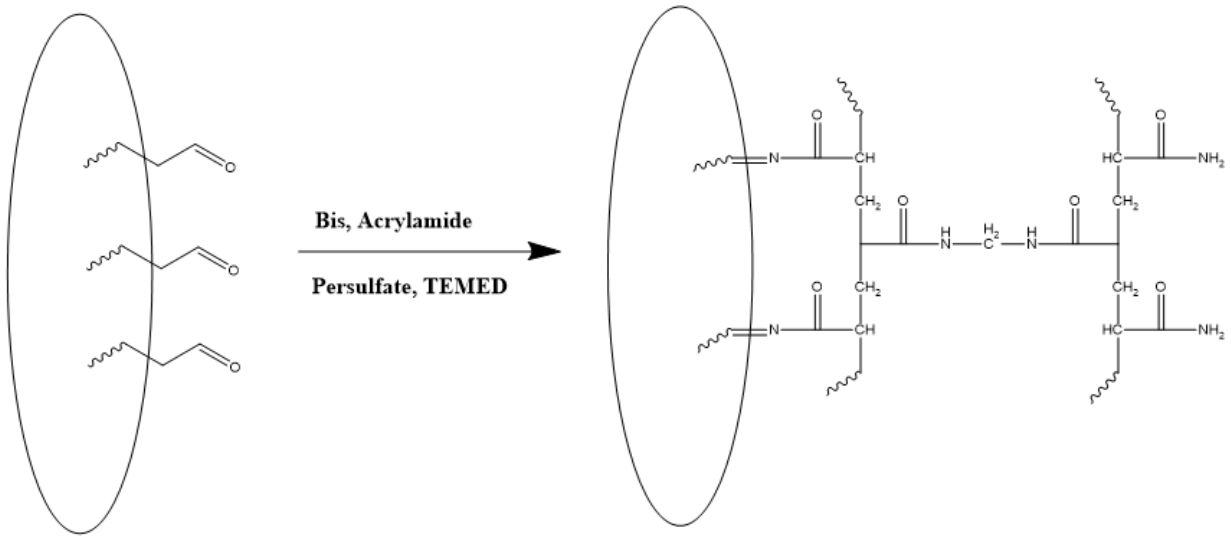

Figure 2. 4 – The aldehyde groups on the coverslips participate in radical polymerization with the acrylamide groups and anchor polyacrylamide gel onto the coverslip.

After roughly 20-25 minutes, the gels will form, verfied by conraction of gel mixture on the edges. Carefully remove the gel from the microscope slide using forceps and then place the formed gels into well plates for further modification. While detaching the gels, fully gelated hydrogel structures will exhibit dendritic delamination from the hydrophobic microscope slide.

After the polyacrylamide hydrogels are formed on coverslips, they are further treated with 1mL of 55% aqueous hydrazine for 2 hours to activate the unreactive amide to a hydrazide that can then react with activated proteins. The activated hydrazides are then washed with glacial acetic acid for 1 hour and then DI water for another hour[58].

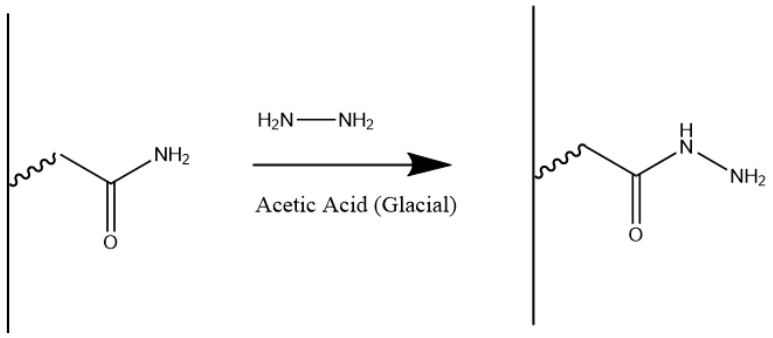

Figure 2. 5 – Depicts the final treatment to functionalize unreactive amide to hydrazides to react with activated matrix proteins

2.2.3 – *Pattern fabrication and gel patterning*

Matrix proteins that will attach to the activated polyacrylamide surface are first activated by oxidizing using sodium periodate. Adhering proteins such as fibronectin, type I collagen or laminin are prepared at 25ug/mL in PBS with 30 minutes of oxidation from sodium periodate at 3.6mg/mL. Stamps of polydimethylsiloxane (PDMS) with positive patterns that have been cleaned with ethanol, water, dried, are coated with the protein mixture for 45 minutes. The stamps are then dried with air and stamped onto hydrogels (Figure 2.6).

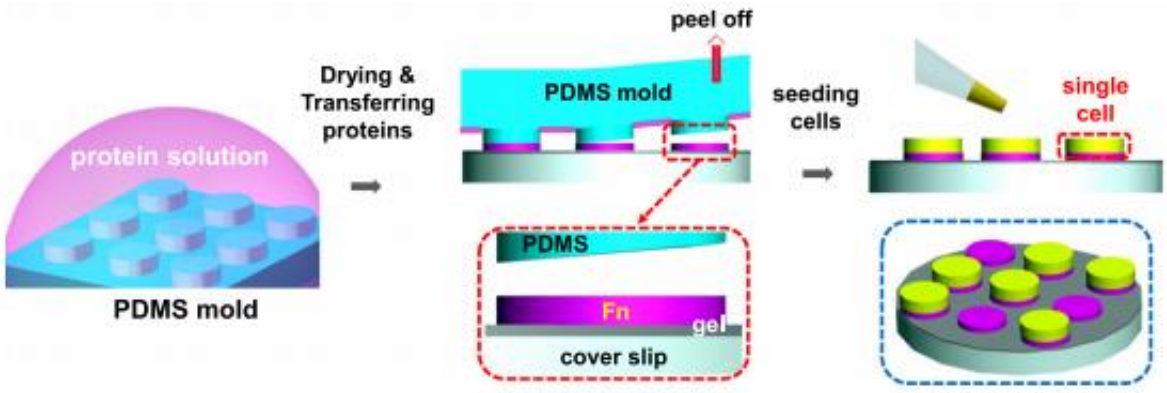

Figure 2. 6 – This schematic demonstrates the patterning process from coating PDMS stamps with activated proteins, to microcontact printing, to the seeding process of single cells on the protein attached patterns [59]. Reprinted from Journal of the Mechanical Behavior of Biomedical Materials, 28, Junmin Lee,Amr A. Abdeen,Tiffany H. Huang,Kristopher A. Kilian, Controlling cell geometry on substrates of variable stiffness can tune the degree of osteogenesis in human mesenchymal stem cells, 209-218, 2014, with permission from Elsevier.

2.3 Results

Proper technique of functionalizing coverslips will allow for polyacrylamide hydrogel synthesis without issues of delaminating and careful micro contact printing will result in precise patterning of desired patterns. When each treatment is successively carried out, proper gel formation is shown in smooth delamination of PA hydrogels (Figure 2.7. These gels are able to stay laminated on coverslips for over a month in PBS or cell medium without altercation to their structure.

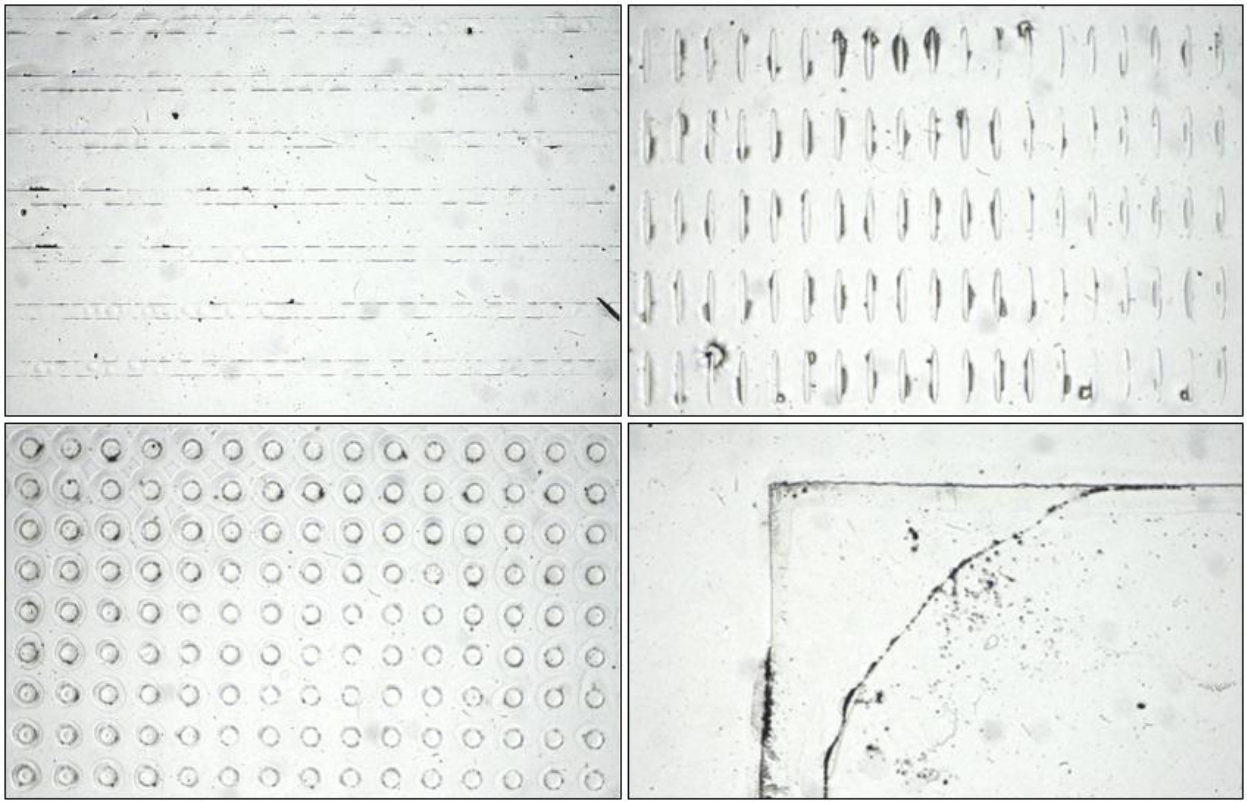

Figure 2. 7 – Successful patterning of polyacrylamide gels result in visible patterns under microscope at 10x. From top left to bottom right, the patterns are of parallel lines at 20uM, 8:1 aspect ratio ovals of 5000um² area, circles of 5000um² area, and the corner of a blank stamp.

To confirm if the patterning was successful with matrix protein, we first used fibrinogen with FITC to verify their adherence to specified patterns shown in Figure 2.8 where the array of circles fluoresced. Next, we wanted to confirm that cells would adhere to these patterned geometries which was shown from MSCs adhering to oval patterns adopting an elongated morphology in Figure 2.8. Lastly, we demonstrate that these patterned hydrogel systems will provide molecular data specifically by staining for molecular structures within

cells verified with staining for the nucleus and cytoskeleton.

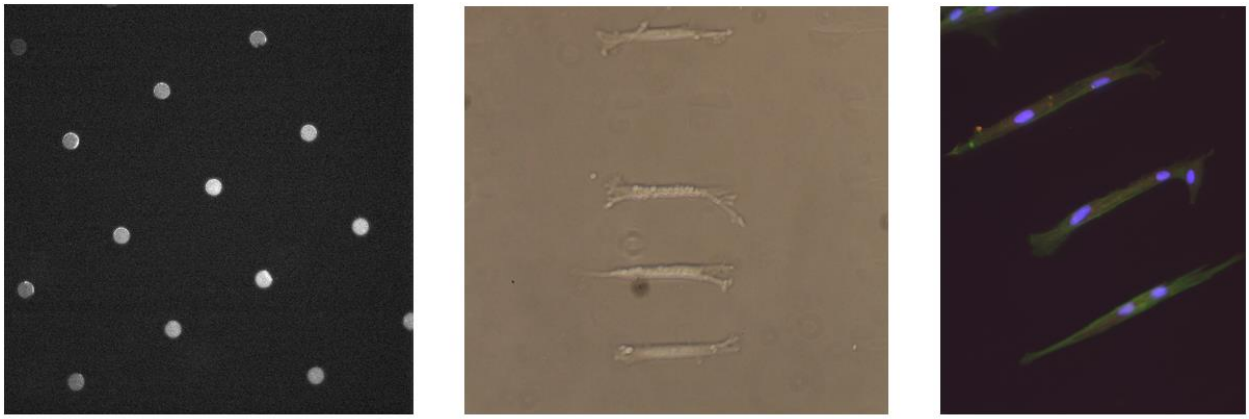

Fluorescent FITC-fibrinogen of circle patterns

Brightfield of cells in oval patterns

Fluorescence: DAPI blue, actin green

Figure 2. 8 – We demonstrate that patterns can be successfully microcontact printed with matrix proteins, where cells would then adhere to, which could provide molecular data on cell behavior and development.

2.4 Discussion

A plethora of hydrogel systems have been developed over the past two decades that incorporate natural and synthetic materials which may incorporate smart properties and elicit particular responses. Functionally, many of these hydrogel systems may be excellent at exploring specific cellular systems or processes in biological applications, but as the hydrogel system is further specified, so will its limitations. For the purposes of studying the mechanotransductive properties of geometry and tissue interfaces, polyacrylamide and polyethylene glycol hydrogels serve as robust materials that allow substrate stiffness modulation and effective patterning with specified matrix proteins[36]. Many biological questions can be explored using these hydrogel systems including the role of tissue to tissue interfaces and the biomechanics involved in natural tissue architecture[60]. For example, patterning on PA gels allow us to create surface architectures that may mimic physiological surfaces such as the sarcomeric bundles seen in cardiomyocytes or the polarized, elongated morphologies seen in neurons[61,62]. These biological insights that can be explored in 2D also provide robust isolation of these mechanical cues; however, it must be addressed that cell systems do exist in complex 3D environments with a myriad of biochemical and physical elements. Biomimetic approach can still simulate aspects of the 3D environment using 2D substrates by simulating both topography and stiffness for robust observation seen in the work by Lee et al. where they report sufficient differentiation with these parameters[30]. As the field rapidly progresses with new insights made in mechanotransduction frequently, the need to mimic combinatorial elements will surface, but the current understanding of many cellular functions still prompts the utility of patterned hydrogels to further develop bioassays specific to single mechanical cues in cellular function and development.

Having prepared and confirmed this system we next sought to use it to study the effects of lipid mediators on MSCs.

Chapter 3

Supplementing mechanotransduction on PA hydrogels with lipid derived molecules to direct lineage specification

In this chapter, we aim to use our developed 2-D polyacrylamide model system to study the effects of various lipid derived molecules on MSC fate in vitro.

3.1 Introduction and Motivation

3.1.1 – *Biological motivation to explore LCPUFA derivatives*

Polyunsaturated fatty acids have been known to exist as signaling molecules and biological products for decades, but elucidation of many of the mechanisms has not been well studied for either lack of knowledge of related pathways that are still being discovered or detection of many of these molecules that are readily hydrolyzed[63]. Although many of these long chain polyunsaturated fatty acid (LCPUFA) derivatives have shown preliminary effects and are not mechanistically well understood, many are entering the market as supplements or treatment for depression, ischemia, blood pressure, and more[64,65]. As the LCPUFA derivatives exist in different isomers, their function and availability differ amongst cell types and diseases. The increasing interest in these molecules open an exciting door to possibilities in future therapies, but also prompts a need to carefully examine the existing uses of these molecules.

3.1.2 – *History of lipid derived molecules*

Unknown to researchers was the utility of derivatives found in Cannabis Sativa such as tetrahydrocannabinol, anandamide, 2-arachidonylglycerol (2-AG) and more which were the first class of lipid derivatives studied. Since then, it has been shown that anandamide and 2-AG play important roles in neuroprotection, antinociceptive and anti-inflammatory pathways validated by studies where

dysregulation of anandamide and 2-AG causes nociception, emotional disorder, neurodegenerative disease, cancer and cardiac disease[66]. As early studies of these molecules demonstrate the wide range of effects they had in different adult cell lines, it is only logical to question how these lipid derived molecules play a role in stem cell biology.

3.1.3 – *LCPUFA derived molecules in neurogenesis from MSCs*

In particular, a class of fatty acid derivative called eicosatrienoic acids has been gaining attention for its association with neurogenic pathways, particularly by acting through the HO-1-pAKT signaling. AKT complexes[67]. The AKT complexes are serine or threonine kinases that bind to PIP3 which is activated by lipid kinase PI3K which then translocates to the membrane. Once activated, AKT phosphorylates many downstream substrates that regulate cell behavior and maintenance. Some of the related pathways include mTOR signaling promoting cell growth and protein synthesis, inhibitory phosphorylation of GSK3 promoting cell cycle progression, Wnt signaling, and formation of neurofibrils. 14, 15-EET is only one specific lipid derived isoforms of cytochrome P450 epoxygenase that has shown its effect on stem cell development towards neurogenic specification.

Widely commercialized supplement docosahexaenoic acids (DHA) have shown to promote neurite growth as well as synaptogenesis in embryonic hippocampal neurons which supports clinical observations of DHA improving memory and learning functions. A study of N-docosahexaenooylethanolamide (DEA), a derivative of DHA, has shown to play significant role in synaptic function in the hippocampus[68]. To distinguish the primary bioactive fatty acid, it was shown that DEA promoted hippocampal neurite growth at much lower concentrations than DHA whereas DEA increased expression of synapsins and glutamate receptors exhibiting increased glutamergic synaptic activity. Furthermore, DEA was shown to encourage neurogenesis in the dentate gyrus of hippocampus suggesting interplay between lipid derived molecules and neurogenesis[69].

3.1.4 – *Exploring the role of lipid derived molecules in adipogenesis*

Many of the lipid derived molecules interact with PPARg, a nuclear receptor of a receptor superfamily that is heavily associated with adipogenic genes, as it is well documented that PPARg along with C/EBp family control adipocyte differentiation[70]. As the PPAR's are a nuclear receptor supefamily that act as orphan receptors, they are activated by many fatty acids and prostaglandins. While PPARg1 is found ubiquitously, PPARg2 is expressed only in adipocytes. DNA binding domains anchor PPAR to a target binding site on DNA via two zinc fingers with retinoic X receptors to direct PPAR response elements. This complex will react with different cofactors, phosphorylate different serine and threonine, and regulate the localization of active PPARs to regulate the genetic landscape that is controlled[71].

As mentioned previously, PPARs is part of an important receptor family that interact with many lipid mediators through the GPCR to serve as a lipid sensor. Some very common fatty acid derivatives might be linoleic acid and arachidonic acid which may act through the COX pathway to activate PPARg. The COX enzymes produce prostanoids that are amino acid derived are PGDs and PGEs.

CYP450 is a common epoxygenases that utilizes many of these lipid substrates make them ideal for generating PPAR ligands. They have lipoxygenase and hydroxylase activities and can degrade steroids, vitamins, and fatty acids to form metabolites that serve as PPAR ligands.

3.1.5 – *Strategies to potentiate effect of lipid derived molecules in stem cell differentiation*

Since the first case of cellular reprogramming to the generation of induced pluripotent stem cells, there has been a lot of excitement with the potential of using a synthetically derived pluripotent cell type without the need to extract embryonic cells[72]. Although there has been many improvements since the first protocol by increasing the efficiency of reprogramming to the use of more robust viral combinations or optimized existing protocols, or even to the use of small molecules, using viral

methods to transduce transcription factors into the genome provides obvious clinical risks[73]. Particularly, the overexpression of these genes can eventually impede normal cellular function or even develop into tumorigenic cells if pro-oncogenes inhibitors are bypassed[74]. The general need for safer methods for reprogramming is definitely required if these technologies are to make it to clinical relevance with autologous usage one day. In the past few years, various groups have shown that a mixture of small molecules that activate similar machinery as the transduced transcription factors can also successfully reprogram somatic cells to near pluripotency or a quasi-pluripotent state; however, many of these protocols have very low reprogramming rates[75]. More frequently is the need to couple these small molecules with viral plasmids for optimized reprogramming.

In addition to the exciting advent of reprogramming, researchers have also demonstrated direct transdifferentiation of pluripotent-like states to another somatic cell, or even more recently demonstrated somatic to somatic reprogramming[76]. Similarly, many of these methods require the use of viral transduction of transcription factors to overexpress specific lineage specific genes to bring about the differentiation and maturation of the target cell type. Recently, there has been methods to induce direct reprogramming of somatic cells using just a cocktail of chemicals.

Cheng et al. has shown successful direct reprogramming of mouse embryonic fibroblasts to neural progenitor cells (NPC) using a chemical cocktail composed of valporic acid, CHIR99021, and Repsox. The chemically derived NPCs showed close resemblance to mouse brain-derived NPCs in regards to their proliferative ability, gene expression, and multipotency as a progenitor cell. The study concluded that a chemical cocktail of a histone of deacetylase inhibitor, glycogen synthase kinases, and TGF-B inhibitor can effectively induce direct reprogramming in hypoxic condition[77].

With evidence that these lipid derivatives play an important role in both adipogenic and neurogenic pathways, coupled to examples of direct reprogramming exhibited by a cocktail of chemicals, it

prompted the question of whether a transformation can further be induced by introducing physiological mechanical cues from hydrogels. As the mechanical environment has shown to play an important role in lineage specification, a combinatorial approach of adding these chemical factors may further encourage lineage specification of mesenchymal stem cells to different fates[78]. Such an approach is one that was considered for this experiment, postulating that the introduction of histone deacetylase inhibitors would loosen the epigenetic landscape of the MSCs for downstream signaling molecules to act on the genome once these lipid derivatives interacted with the MSCs. Furthermore, a loosened epigenetic state would amplify the mechanotransduction cascade experienced on a physiological substrate and encourage lineage specification towards the cell type that would likely exist in a similar environment.

3.1.6 – *Selecting HDAC inhibitors to augment differentiation*

Finally when planning for the lipid panel experiment, we noted that HDACi's can potentiate the role of the lipid derived molecules for MSC differentiation to loosen the epigenetic landscape and increase pluripotency genes[79,80,81]. It was also interesting to note that HDACi's have been utilized in neurogenic studies both on cell cultures and in animal models previously. Kim et al. demonstrated that sodium butyrate (SB) introduced in ischemic brain stimulated neurogenesis[82]. They demonstrated that SB increased polysiliac acid-neural cell adhesion molecules, nestin, GFAP, CREB, and BDNF. In another experiment, George et al. report TSA and VPA improved post-stroke neurogenesis in the dentate gyrus of hippocampus validated by the increase incorporation of BrDU[83]. Interestingly, although neurogenesis in the DG of hippocampus may have been increased by TSA, Shaked et al. report that TSA decreased neurogenesis in glial cells[84]. They demonstrate that class I and II HDACs inhibit BMP2/4 expression in glial cells which serves as a modulator switch

from neural cells to astro/glial cells. This prompted us to choose the HDACi's of SB and VPA to further potentiate the role of lipid derived molecules on possible genetic or epigenetic controls.

3.2 Materials and methods

3.2.1 – *Testing dose dependent effect of lipid derived molecules*

As many long chain polyunsaturated fatty acid (LCPUFA) metabolites exist, we decided to investigate the effects of epoxy derivatives of omega 3 fatty acids synthesized by cytochrome P450 (CYP) such as 14, 15 – epoxyeicosatrienoic acid (EET), 19, 20 – epoxydocosapentaenoic acid (EDP) and a potent lipid steroid dehydroepiandrosterone (DHEA) on MSC development (structures can be seen in Fig 5.X). The LCPUFA derivatives and DHEA were synthesized and provided by Dan McDougle from the Aditi Das group in the department of Biochemistry at the University of Illinois at Urbana Champaign.

This first investigation utilized the lipid molecules and a hydrogel substrate mimicking the substrate elasticity of our target cell types of adipocytes or neurons. To begin, PA hydrogels of 1kPa were synthesized on glass coverslips. On glass coverslips treated with APTS and gluteraldyde, the PA gels were mixed with the initiator, then 20 uL was pipetted onto hydrophobically treated glass slides, and then sandwiched with the glass coverslip. After 25 minutes, the coverslips were detached from the slides with the formed gels, and then treated with hydrazine and glacial acetic acid. The gels were patterned with a blank stamp of activated fibronectin.

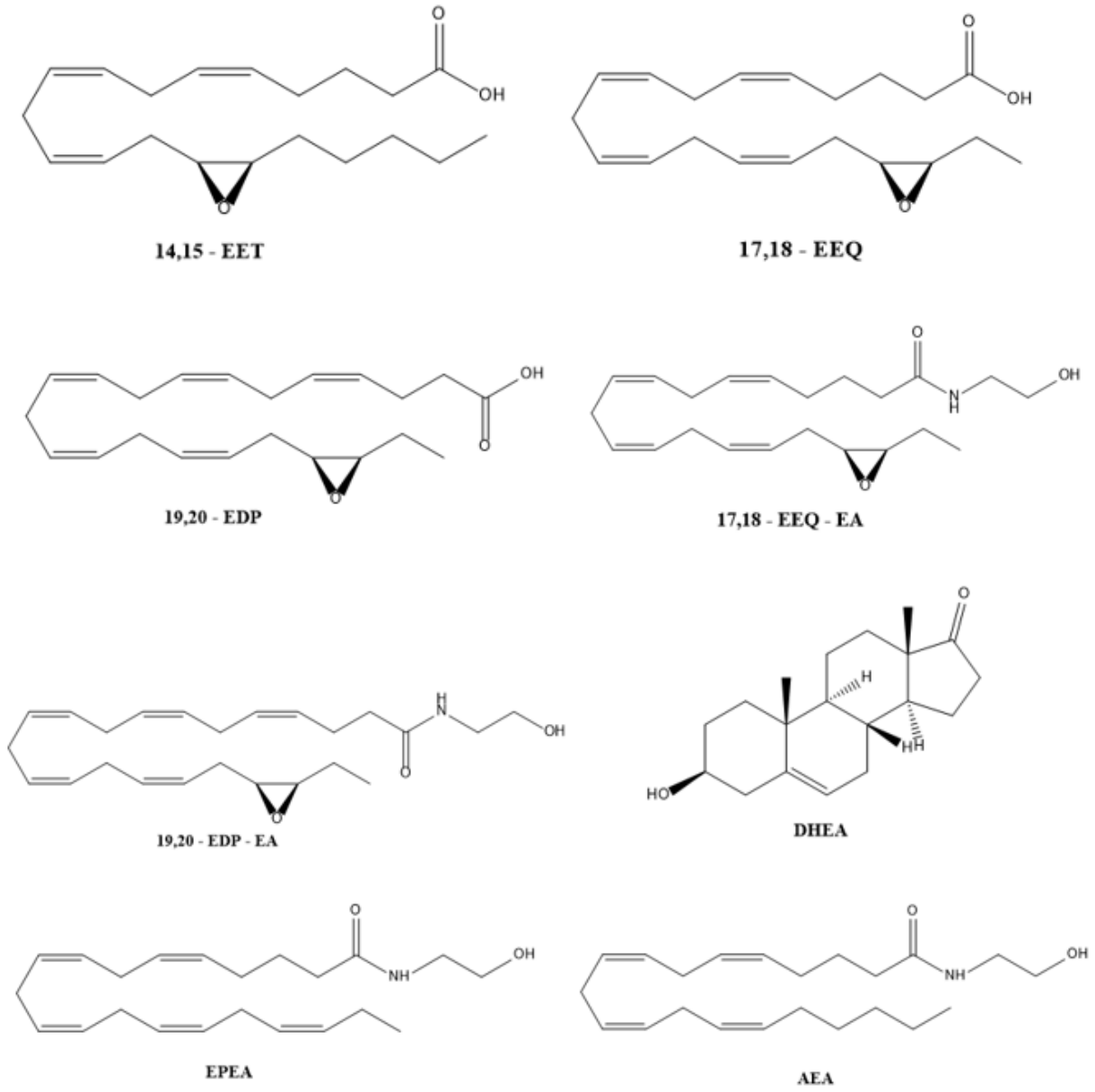

Figure 3. 1 – The figure above depicts the structures of the long chain polyunsaturated fatty acid derivatives that were used for this experiment.

The first experiment sought to understand if there were any concentration dependent effects with this lipid molecules. For 14, 15 – EET, we tested concentrations of 100nM, 300nM, and 3uM while we tested concentrations of 100nM, 1uM, and 9uM for both DHEA and 19, 20 – EDP. For each molecule, we tested the vehicle control of EtOH for EET and DMSO for DHEA and EDP.

Culture dishes that were culturing MSCs were trypsinized and passaged onto the gels once they reached confluency at ~ 30,000 cells per well. Using roughly one confluent 10mm dish per three 12 well plates, cells were suspended in MSC media and then passaged onto the gels. After initial seeding, each well plate was observed under microscope to ensure attachment of MSCs to their substrate. Checking after 1 hour, it was evident that cells were attached to the fibronectin. During the time the cells were attaching onto the gels, serum free media was warmed in the water bath to introduce the lipids. Suspended in the appropriate vehicle, lipids were added into serum free media into 15mL media tubes to the desired concentrations. After about three hours of initial seeding, the MSC media was replaced with the serum free media for twelve hours. During this time, MSC media was aliquoted to 50mL centrifuge tubes to make media with the three different lipids at three different concentrations. After the twelve hours, the serum free media was replaced with MSC media with the lipids. After the initial twelve hour exposure to the serum free media, cells were fixed after three days, ten days, and fourteen days with media changes every three days.

3.2.2 – *Lipid panel assay*

After conducting the initial experiment with the lipid molecules and verifying differences in marker expression based on molecules and substrates, we were interested in conducting a panel study with a variety of lipid molecules to observe if any of the molecules had significantly distinguishable expression on physiological substrate stiffness. Taking the results from the first experiment, we saw increased expression of MAP2 and PPARg at day 3; however, there was concern that the increased expression may have been to effects of trypsin. In the following experiment, we wanted to also investigate the effects of histone deacetylase inhibitors (HDACi) which may loosen the epigenetic landscape and potentiate the effects of the lipid molecules. Furthermore, literature also suggested sodium butyrate and valporic acid had shown increased neurogenesis in the SGZ in the hippocampus when treating mice[85].

For the panel experiment, there were eight lipids provided by the Das group. The eight lipids were 14, 15-EET (suspended in DSMO), 17, 18-EEQ (suspended in DSMO), 19, 20-EDP (suspended in DSMO), 17, 18-EEQ-EA (suspended in DSMO), 19, 20-EDP-EA (suspended in DSMO), EPEA (suspended in DSMO), DHEA (suspended in DSMO), and AEA (suspended in DSMO). Since the previous experiment showed no cytotoxicity for concentrations of 9uM, we decided to use a concentration of 10uM for each molecule.

Before introducing the HDACi's to the MSCs in conjunction with the fatty acids, two precautionary experiments were conducted to test the cytotoxity of HDACi's and serum free media. In a 12 well plate with MSCs seeded, serum free media was introduced after three hours of seeding in MSC media. The first three columns were changed to serum free medium and the last column was left as a control in MSC media. After 6 hours, the media in the first column was changed to MSC media, the second at 12 hours, and the third at 24 hours. Then after three days, the MSCs were observed for viability. After validating the viability of MSCs in serum free medium, another experiment was conducted to see what concentration may cause cytotoxicity. In serum free medium, concentrations of VPA and SB were made at 0.5mM, 1mM, and 5mM in a similar set up.

From the results of the two side experiments, it was shown that concentration of 5mM exposed for 18 hours showed no cytotoxicity to MSCs checked after three days, but to ensure maximum viability, a concentration of 1mM was chosen with 12 hour exposure. For this experiment, PA hydrogels were patterned with blank patterns of fibronectin, and then MSCs were seeded with MSC media at ~30,000 cells per well. After three hours, serum free media with 1mM of VPA or SB was added for 12 hours, with 10uM of lipid molecule. After 12 hours of exposure to serum free media with HDACi's, the media was changed to MSC media with the same concentration of fatty acid. After six and nine days

of culturing on the gel with media change every three days, the cells were fixed, stained with beta III tubulin, and then imaged using an GE in-cell analyzer 4000.

3.3 Results

3.3.1 – *Investigating dose dependent response of lipid molecules*

After analyzing the fluorescent images from staining from the first lipid derived molecule experiment, it is evident in the expression of both MAP2 and PPARg that relative intensity of each marker was highest on day 3. In the 14, 15 – EET experiment, there was a dose dependent effect of the small molecule MAP2 and PPARg expression on day 3; however, in day 10 and 14, no noticeable dose dependence increase was observed on cells seeded on gels compared to control glass substrates. In DHEA and 19, 20 – EDP scenarios, dose dependence on significantly different expression of markers is not observed from gel and glass except for PPARg expression for DHEA on day 3 where an inverse dose dependent trend is observed where PPARg expression decreased with increasing concentration. Although dose dependence of the small molecules may not be observed among most conditions, it is evident that these lipid molecules demonstrated increased marker expression when cells were seeded on gels of physiological surfaces.

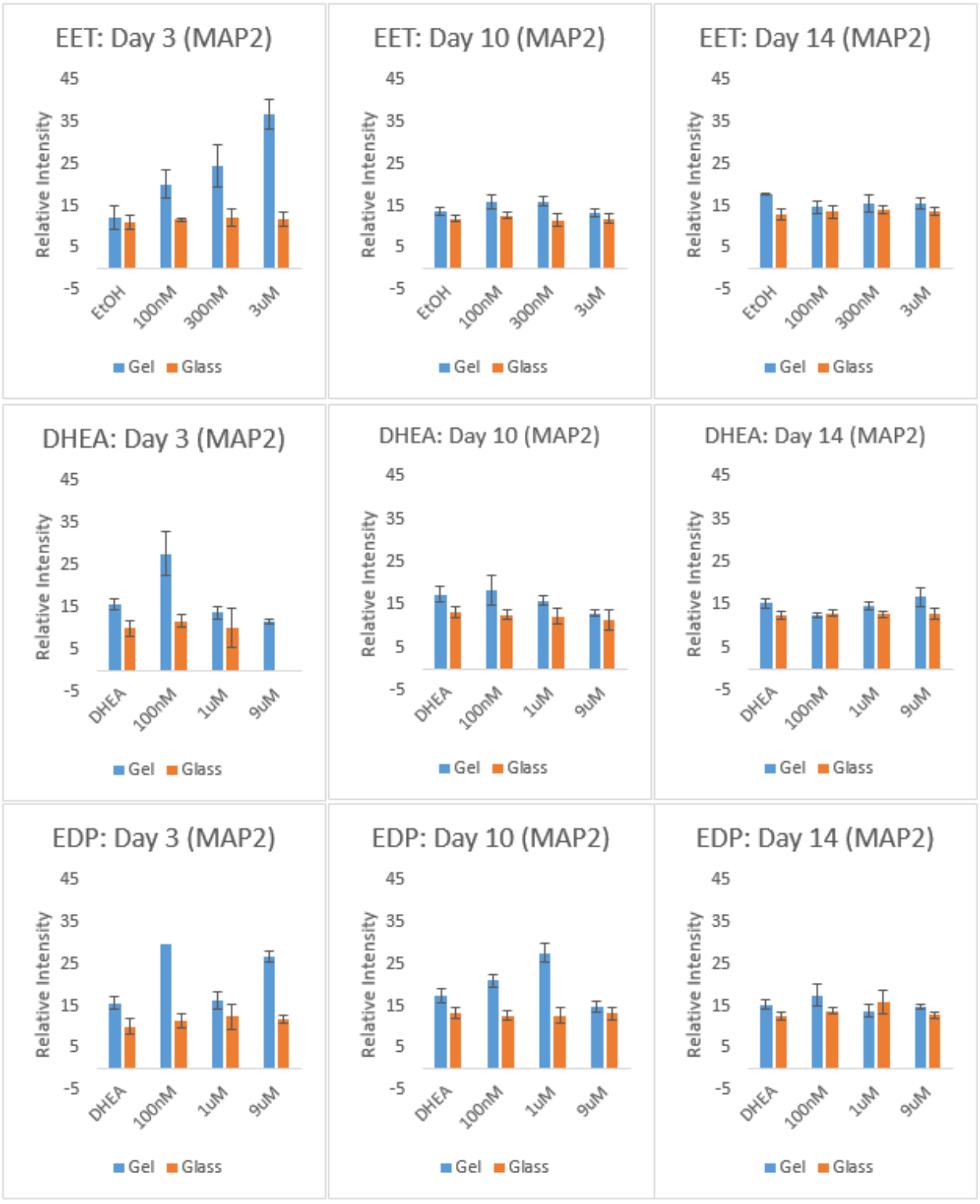

Figure 3. 2 – A comparative study investigating the temporal and dose dependent effect of these lipid derived molecules on the expression of MAP2 on both gel and glass substrate.

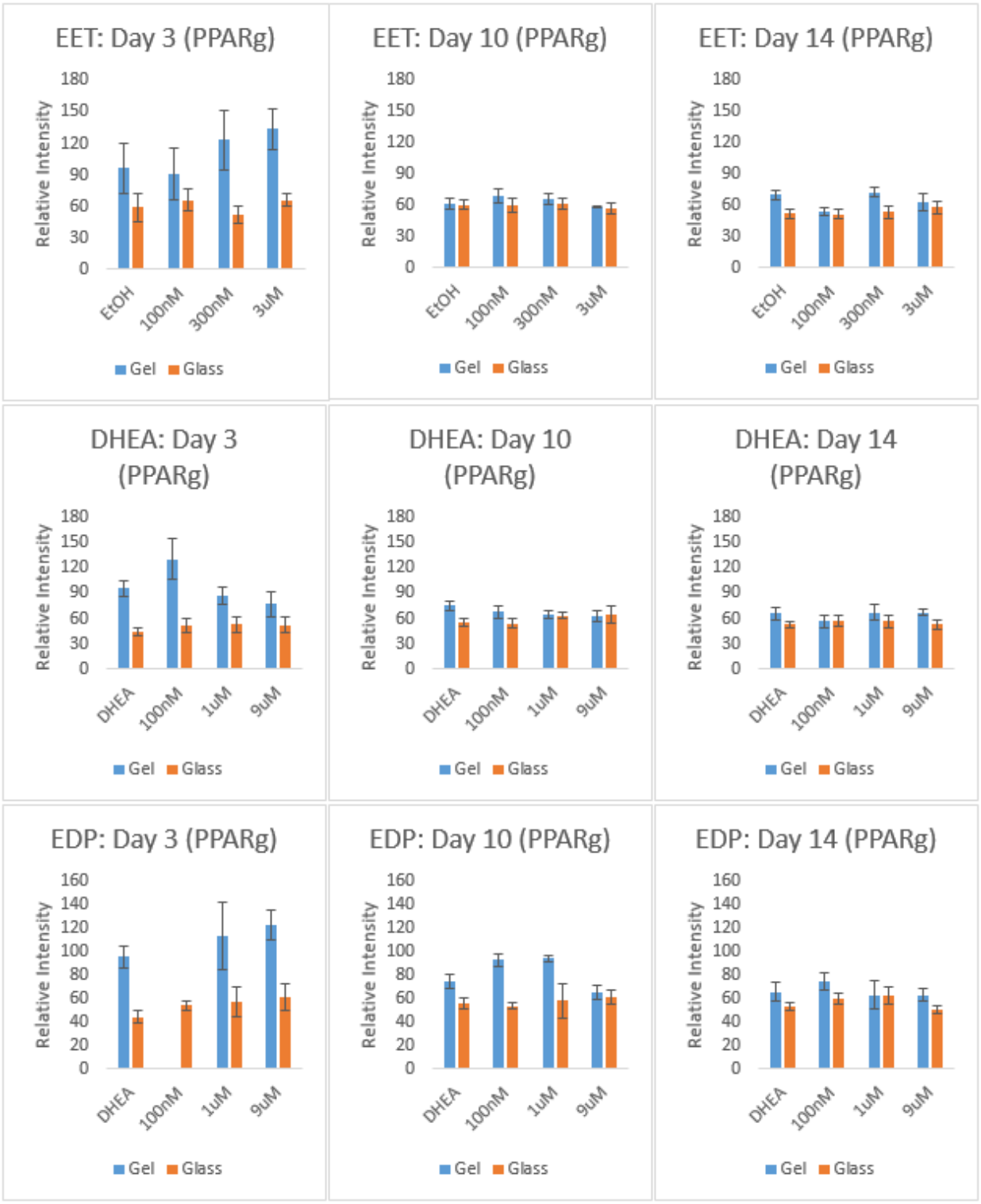

Figure 3. 3 – A comparative study investigating the temporal and dose dependent effect of these lipid derived molecules on the expression of PPARg on both gel and glass substrate.

The first experiment demonstrated that lipid derived molecules in conjunction with physiologically relevant substrates yielded different biological responses, possibly suggesting increased lineage specification towards an adipogenic or neurogenic fate. This prompted the second experiment investigating which specific lipid derived molecules may demonstrate increased marker expression. It is very interesting to note that many of the small molecules demonstrated temporal differences in the expression of such markers. This can be observed clearly in the control samples where samples are not treated with lipid derived molecules, but merely treated with the HDACi's, carrier, and MSC media. The expression level of both markers change temporally amongst all samples where the ratio of expression seems to favor PPARg at day 6, but competes with intensity for B3 tubulin on day 9. Further temporal differences can be observed in the expression of B3 tubulin in both HDACi scenarios. Samples treated with SB show increased expression for 17, 18 – EEQ and 19, 20 – EDP on Day 9, but decreased expression for 19, 20 – EDP-EA and EPEA. When samples are treated with VPA, there is high expression of B3 tubulin on Day 6 for 19, 20 – EDP and 17, 18 – EEQ-EA, but lower expression on day 9. It is also interesting to note that in SB treatment, 17, 18 – EEQ and 19, 20 – EDP show increased expression of B3 on gels, whereas VPA demonstrate decreased expression on gels compared to glass. Also comparing SB and VPA treatment, 19, 20 – EDP-EA and EPEA showed decreased expression on gels compared to glass for SB treatment, but no statistically different expression on VPA treatment suggesting different HDACi's correlate to different changes in lineage specification.

3.3.2 – *Lipid panel experiment*

By assaying the expression of early neural fate marker B3 tubulin and adipogenic control PPARg, we found interesting differences among the panel of lipid derived molecules. Seen in the control samples, the different HDACi's showed varying responses between each other, but showed temporal differences. On day 9 of the experiment, we saw higher expression of in both markers from DMSO and gel condition with MSC media. Comparing the relative intensity, expression of PPARg from VPA and SB remained relatively similar from days 6 and 9, but we saw that DMSO increased nearly five-fold for PPARg expression suggesting that the vehicle may also have an influence in conjunction with the lipid derived molecules.

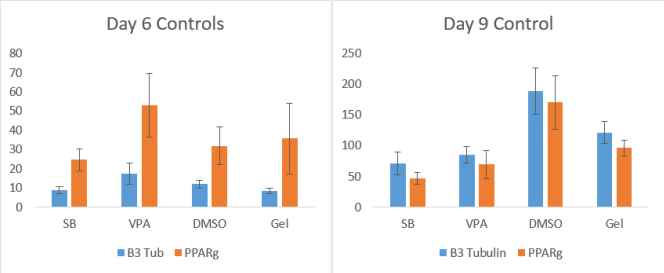

Figure 3. 4 – Controls were ensured to validate the differences of the HDACi's and vehicle for both B3 Tubulin and PPARg expression.

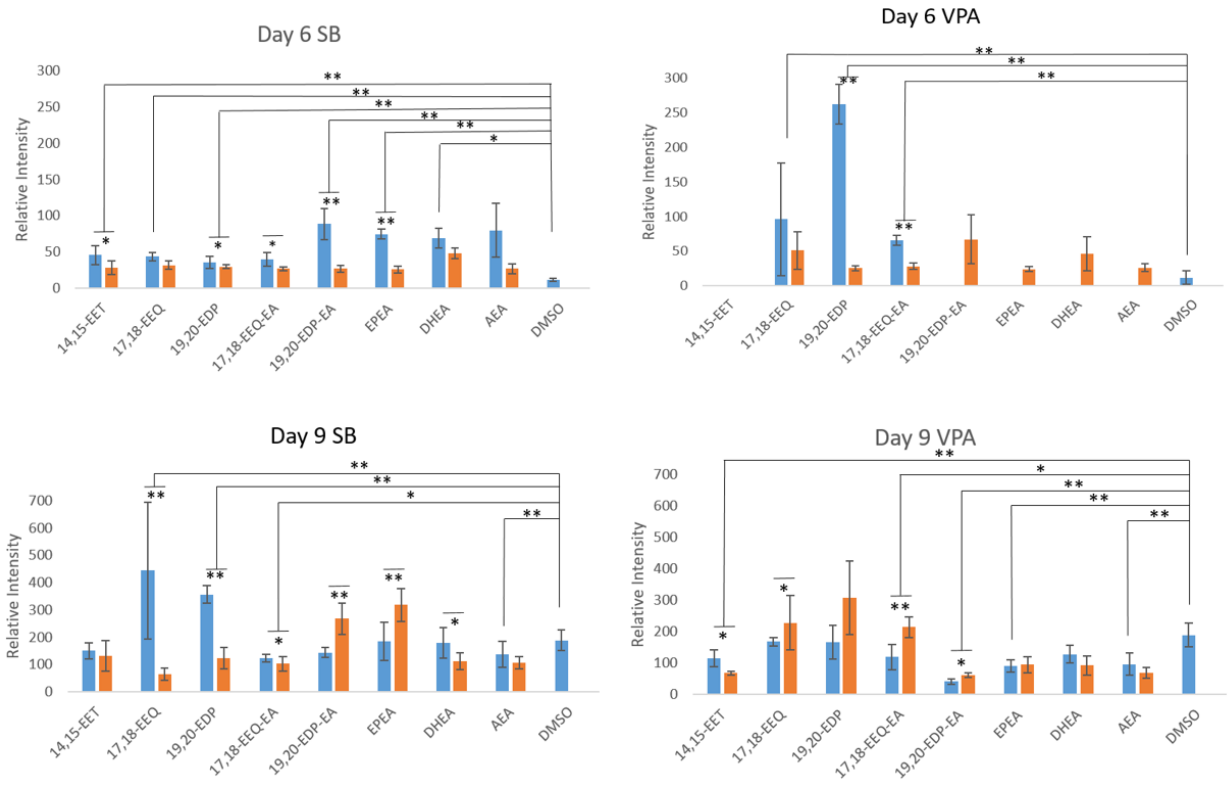

*Figure 3. 5 The expression of B3 Tubulin from the lipid panel experiment. * denotes P < 0.05 and ** denotes P < 0.01. The blue bars represent the samples that were on gel and the orange bars represent samples on glass.*

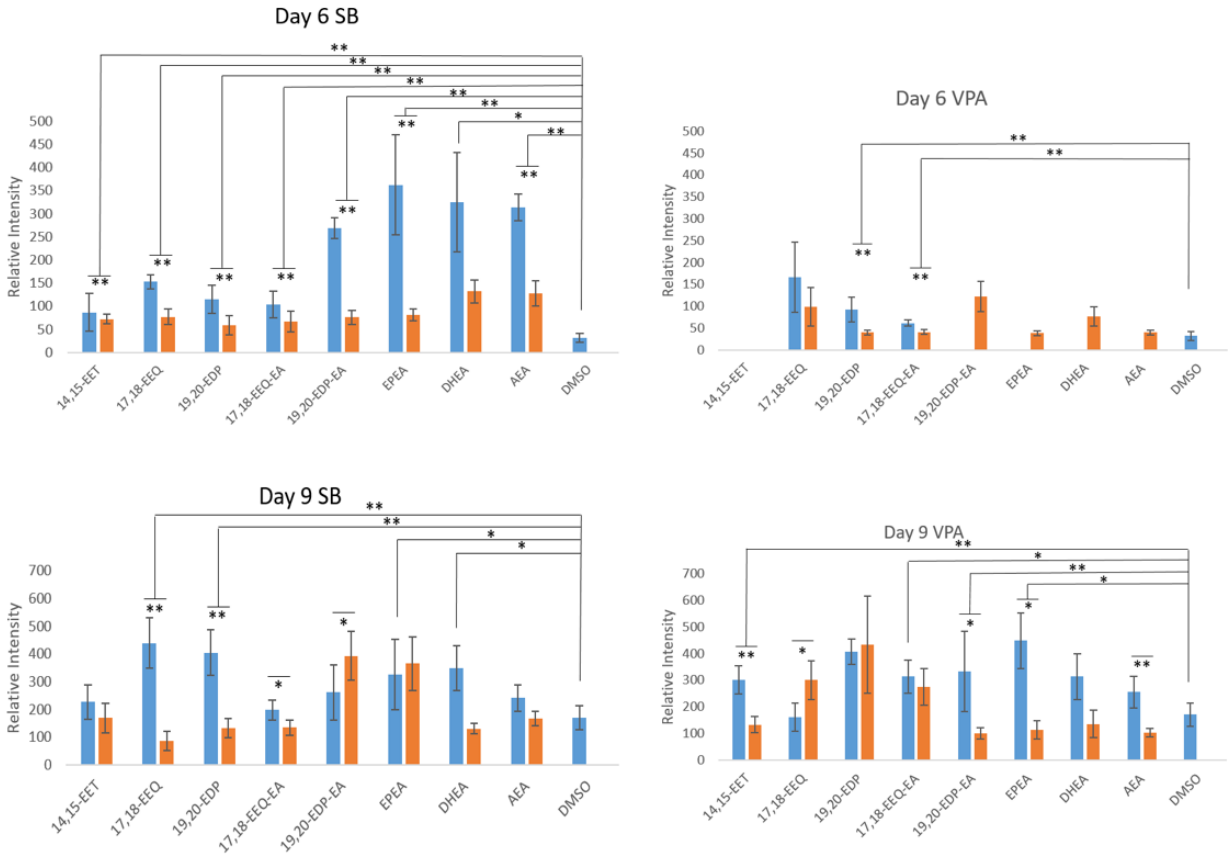

*Figure 3. 6 – The expression of PPARg from the lipid panel experiment. * denotes P < 0.05 and ** denotes P < 0.01. The blue bars represent the samples that were on gel and the orange bars represent samples on glass.*

In the expression of PPARg in the SB and VPA treated samples, there is a similar trend observed between both HDACi's and a theme of temporal differences is also conserved in PPARg expression. Observing the temporal differences in SB treated samples, we can see a drastic drop in PPARg expression in 19, 20 – EDP-EA, EPEA, DHEA, and AEA from day 6 to 9 whereas PPARg expression drastically increased 17, 18 – EEQ and 19, 20 – EDP from days 6 to 9. Comparing the expression between both HDACi's, statistically increased expression from 17, 18 – EEQ and 19, 20 – EDP in SB treated samples are not mirrored in VPA samples whereas statistically increased expression from 19, 20 – EDP-EA and EPEA in VPA treated samples are not mirrored in SB samples. Although further biological insight is limited without further mechanistic studies, it is interesting to note that expression levels of both B3 tubulin and PPARg differ temporally and between HDACi's when

compared on physiological stiffness and glass. Unfortunately, few samples in the VPA treated condition on day 6 exhibited poor resolution when imaging preventing any quantifiable intensity to be measured. Relative intensity of the marker expression on glass for these conditions can provide clearer comparison on HDACi influence on marker expression and temporal comparison to further validate the observations made above.

3.4 Discussion

The first experiment testing dose dependence of lipid derived molecules had interesting increase in expression early in the process occurring at day 3. This observation may have occurred for two reasons. When the samples were fixed on an earlier time point, the serum free media devoid of soluble epoxide hydrolyzes or other enzymes that break down the lipid molecules may have had increased potency of molecule signaling. As reports suggest the sensitivity of these lipid derived molecules to respective hydrolases, effectivity of molecules may be reduced significantly in later time points. Secondly, this increased expression early on may be attributed to the effects of trypsin. As trypsin cleaves MSC attachment from tissue culture plastic attachment sites to matrix proteins on the gel, cells undergo a change in morphology from spread out spindles to balled spheres, until they reform their contractile cytoskeleton after adhering to matrix protein.

After concluding that these lipid derived molecules demonstrated differences in marker expression when seeded on different substrates, we conducted a second experiment assaying expression of B3 tubulin and PPARg for eight lipid derivatives. Although it was unfortunate that a few samples were not able to be measured, the trends were evident from the existing fluorescence data. Temporally, there were differences between each time point, and between each HDACi's, there

were differences in expression for particular lipid derived molecule. When considering the difference in expression that occurred temporally, it was found that these differences usually occurred for lipids 19, 20, EDP-EA, EPEA, DHEA, and AEA. When considering the difference in expression that occurred between HDACi's, it was found that marker differences occurs for lipids 17, 18 – EEQ, 19, 20, EDP, 19, 20, EDP-EA, and EPEA.

When searching the literature regarding the role and effect of these lipid derived molecules, many of them elicit a broad range of responses either through cell studies, animal studies, or even in clinical trials. Although further expansion on the mechanism may be difficult to completely ascertain regarding the observations made in this experiment, we can speculate some possible roles that the drugs played during the development of the MSCs.

14, 15 – EET: This lipid derivative is often associated with vascular functions and often coupled to its ability to dilate vasculature, cause anti-inflammatory cascades, and induce angiogenic effects. Although a large body of evidence in peripheral tissue suggest a role for these EET's, its action in the central nervous system (CNS) seems to also parallel neuro-vascular coupling relationships in the CNS. Iliff et al. demonstrate that EETs play a role in cell-cell communication in the CNS coordinating responses between different cell types[86]. Further investigating on the mode of activation, they found that EETs activate a specific GPCR regulated by the PKA pathway. This can also further explain the Ca2+ sensitive K+ channels that modulate vasomotor responses. Although interesting to note is the interconnected of these lipid species to create these derivatives as Iliff demonstrate that AEA and 2-AG both serve as substrates for CYP epoxygenase where AEA specifically attribute to CYP-3A4 isoforms found in microglial cells and AEA attribute to CYP-4X1 found in brain to convert to 14, 15-EET-EA. Lastly, they prescribe that 14, 15–EET's are potent activators of PPAR signaling that may also reduce oxidative stresses in hypoxic/ischemic environments[87]. These results are further supported

by Wang et al. who report 14, 15-EETs protected neurons from apoptosis by promoting mitochondrial biogenesis to mitigate ischemia through CREB activation from PPARg[88]. Interestingly, Chen et al. shows 14, 15-EETs as molecules to encourage thymidine incorporation and induce mitogenic effects whereas no CYP metabolites showed a similar response[89]. This study also demonstrates 14, 15-EET demonstrated increased proliferation with upregulation of c-fos and egr-1 mRNA which are mechano-sensitive regulators of the AP-1 pathway during cell proliferation. This suggests a role for the physiologically relevant substrate in conjunction with the molecule to potentiate responses in cell proliferation possibly to create networks of developing neural-like cells. The role of 14, 15-EETs is not limited to oxygen regulation and proliferation, but has also been implied in neurogenesis. Yuen et al. demonstrate that 14, 15-EETs elevated expression of brain derived neurotrophic factors shown to protect astrocytes oxidative stresses by activating regulatory mediators through the PPARg and CREB pathways[90]. Although many of these studies have been conducted on mouse models, Kim et al. demonstrate that hMSCs express high level of CYP2J2 which actively synthesize EETs[67]. When soluble epoxide hydrolases (sEH) are inhibited in the environment, they showed decreased abiogenesis and that result is also mirrored in our day 6 expression levels of B3 Tubulin in SB treatment. Although our data regarding the temporal expression of PPARg and B3 tubulin may not capture the full picture of its effect on MSCs on mechanically compliant surfaces, the diverse role of 14, 15-EETs in neural protection and function suggest that its effect may be more regulatory than developmental, or if it is developmental it may play a role in late stage neurogenesis.

17, 18 – EEQ: Although EEQ's are not as well studied as the relatively ubiquitous EETs, few studies suggest its role in neural function as well as possible adipogenesis. Shao et al. demonstrated that 17, 18-EEQs increased vascularization through upregulation of VEGF-a specifically[91]. This commonality of lipid derived molecules to encourage angiogenesis and mediate vasodilation show case an important physiological response that is important for neurogenesis[92,93]. Although not directly studied in the

context of neural lineages, it has been shown that 17, 18-EEQ's act as anti-arrhythmic agents by suppressing Ca2+ induced beating similar to a mode of action as EETs shown by Arnold et al[94]. When studied in the context of insulin signaling, it has been shown at 17, 18-EEQ is increased in insulin sensitive tissues which many hepatic associated effects. Furthermore, Vicario et al. demonstrate that it restores functionality of the Atg signaling pathway that eradicates damaged cells skewing the macrophages not to adopt an inflammatory mode of action[95]. Interestingly, they also report that 17, 18-EEQ's increased the mass of brown adipose tissue mass. In our SB samples, we see that the 17, 18-EEQ samples exhibited increased expression from the control increasing from day 6 to 9 suggesting possible correlation to their study.

19, 20 – EDP: The role of these lipid derivatives seem less understood compared to the other epoxy derivatives, and interestingly they exhibit inhibition of angiogenesis. Zhang et al. report that 19, 20-EDP inhibit VEGF and FGF2 to discourage angiogenesis[96]. On experiments with HUVECs, they show that EDP's effectively inhibit angiogenesis and also inhibit VEGF induced migration across fibronectin. Contrary to the study on reduced blood formation, Ulu et al. show that clinical application of 19, 20-EDP decreased blood pressure by the arachidonic acid pathway[97]. In a study of thrombosis, Jung et al. demonstrate that 19, 20-EDP's decrease aggregation of thrombocytes to vascular walls[98]. In SB treated samples, we see increase in PPARg and increase in B3 tubulin in these molecules. It proves difficult to relate the effects of these molecules, to their associated pathways, to marker expression of B3 tubulin and PPARg; however, the large difference in expression between gel and glass does prompt an interesting question on the role of 19, 20-EDPs in mechanically responsive pathways, PPARg pathway and neurogenic pathways.

DHEA: Since the advent of lipid studies, DHA has been studied for neurogenesis in the subgranular zone in hippocampal neurons and showed increased BrdU incorporation. A specific derivative of

DHA is DHEA which also exhibit neurogenic effects demonstrate that it is more potent at promoting neurogenesis by suggesting its regulation the inhibitory effect of corticoids by Karishma et al[99]. Similarly, Moriguchi et al. report DHEA improving neurogenesis in the subgranular zone of the hippocampal dentate gyrus where they observe increased phosphorylation of AKT, ERK, and GSK-3B pathways[100]. Interestingly, ERK is a kinase associated with mechanotransduction where the hydrogel substrates may potentiate the effects of ERK activation[101]. Also suggested in neuroprotective roles, Hu et al. demonstrate that transgenic mice with the fat-1 gene that converts omega 6 to omega 3 PUFAs show less brain damage post induced stroke with improved neurologic function[102]. They observed that this effect occurs through enhanced neural stem cell proliferation and differentiation. We demonstrate that PPARg expression is increased when treated with SB in DHEA conditions and in day 6 for B3 tubulin for SB conditions as well. This may suggest that the role of DHEA may be better complemented with SB, but not as pronounced from VPA.

Interestingly between the samples on gel and glass substrate, not all the B3 tubulin expressions were increased on the gel markers. Lee et al. reported that MSCs seeded on physiologically relevant substrates expressed higher levels of B3 tubulin on day 10 similar to a time point of day 9 for this experiment[30]. In many of the lipid derived molecules, there is pronounced increase expression of markers in day 6 on the gel sample compared to the glass, but molecules such as 19, 20-EDP in and 17, 18-EEQ-EA in VPA treated samples at day 9 and 19, 29-EDP-EA and EPEA in SB treated samples in day 9 show decreased marker expression on gel compared to glass. This suggests that there may hierarchies in signaling occurring within the MSCs where lipid signaling may have more pronounced effects than the mechanical signals received from the hydrogels which posed an interesting question of how these signals may be used in conjunction to target MSCs towards target neural or other desired fates.

The novelty of this experiment is two-fold. First, the mechanistic pathway of many of these lipid derived molecules is not well understood. Many studies will incorporate these molecules in animal studies or empirically observe changes in specific markers, but much is yet to be discovered regarding their mode of action and interconnectedness with developmental pathways. Second, these experiments also showcase that different HDACi's exert different epigenetic changes which drive different lineage preferences. The difference in epigenetic changes that result in different marker expression indicate that the effects of lipid derived molecules are transduced to an epigenetic scale further stressing the importance of understanding the underlying mechanism. Furthermore, the differences in expression seen on hydrogel substrate and glass also suggest interplay between the lipid signaling cascade with the mechanotransductive cascade in MSC models, which can be assumed to play a role in other progenitor cell types in the very least.

Having confirmed our 2-D model system in these experiments, and knowing the importance and differences of 3-D culture compared to 2-D, we next sought to develop a model system suitable for encapsulating cells in 3-D, again focusing on MSCs, but choosing angiogenesis as a model problem.

Chapter 4

3D spatially defined PEGDA based hydrogel co-cultures

In this chapter, we make the move to a 3D PEGDA based model hydrogel in order to study cell-matrix interactions in 3D as well as study cell-cell interactions in a co-culture model.

4.1 Introduction to hydrogel co-cultures

4.1.1 – *A model co-culture: exploring signaling that guides angiogenesis.*

The current trend in angiogenesis therapy seeks to use growth factors such as vascular endothelial growth factors (VEGF) or other cytokines to promote angiogenesis; however, many limitations have compromised the effectiveness of these singular therapies. Several drawbacks of using a single set of factors to promote angiogenesis include irregular blood vessel formation, dilation in existing vessels, or even the promotion of tumors[103]. In recent years, the rise of stem cell therapies has garnered positive attention in the field of angiogenesis where biological limitations of chemical cues may be overcome using the natural secretome of pro-angiogenic cells. Thought to act as pericytes, MSCs can serve as therapeutic agents through complementary secreted factors to encourage angiogenesis[104].

There have been several methods to harness the therapeutic properties of MSCs by controlling aspects of MSC behavior[105]. Attempts to control MSC behavior have been demonstrated by varying aspects of the microenvironment such as the ECM stiffness, composition, and even geometry[78,106]. As discussed previously, the mechanical aspect of the ECM have been demonstrated to affect the secretory profile of MSCs thus suggesting potential use to induce and encourage angiogenesis.

4.1.2 – *Advantages of Co-culture*

Early in cellular research, co-cultures provided an effective means of expanding colonies of cells and maintaining their viability[107]. It has been shown that retaining as much of the cells physiological environment would improve their ability to behave naturally. When cells are cultured with other cells that may be found in their tissue, their secretome is different than that of cultures of a single cell type[108,107]. The crosstalk between cells within tissues is an important aspect that regulates the autocrine, paracrine, and juxtacrine signaling within tissue for its maintenance and function. With this idea, secretory feedback between cells may provide methods to direct a range of cellular processes. For instance, it has been shown that endothelial cells can alter the regulation of genes of MSCs[109,110].

4.1.3 – *Motivation for investigating dimensionality of cocultures*

For therapies that would incorporate MSCs, mimicking the 3-D microenvironment and the complexity of natural tissue would better recapitulate the in vivo tissue thus favoring the secretory profile towards natural behavior[111]. It has been shown that the signaling profile in 3-D matrices are different than 2-D matrices indicating that the dimensional mimicry would enhance cell based therapies[112]. Furthermore, when MSCs are encapsulated in hydrogel matrices, they have shown better viability when transplanted within patients suggesting that 3D matrices better capture the physiological environment for smoother transition and may be necessary to drive angiogenesis.

Here, we explore how mimicry of physiological environments can encourage a physiological process in encapsulated MSCs co-cultured with vascular cells[111]. Matrix proteins are conjugated within PEG hydrogels for the investigation of angiogenic potential for MSCs in 2D and 3D cultures. On a 2D platform, cells will be grown in a well plate whereas the cells grown in 3D culture will require encapsulation.

4.1.4 – *Importance of paracrine factors in cellular maintenance and function*

A major factor underlying the utility and importance of co-culture systems is the ability for cells in physiological environments to regulate function and behavior through paracrine signaling[108]. The cytokines released into the microenvironment of neighboring cells allow sensing of their niche to dictate function. Specific examples of this can be seen in elimination of diseased or damaged cells where the cells targeted for degradation release factors signaling neighboring cells to assist autophagy[113]. In stem cell biology, niche cells have been shown to guide stem cells towards various fates through cytokine signaling such as lung stem cells and the stroma[114]. Regarding the specific cellular process of angiogenesis, it is well known that VEGF expression heavily dictates the ability of cells to proliferate and form new blood vessels, but many cytokines that are differentially expressed in mechanically differing environments can optimize angiogenesis[115].

4.2 Materials and methods

4.2.1 – Comparing dimensionality of culture systems on angiogenesis

This first experiment involved culturing MSCs on two different platforms. For the 2D system, PEGDA was synthesized between a coverslip and microscope slide with a substrate stiffness of 40kPa. Fibronectin was then attached as the matrix protein based on previous work from Abdeen et al[58] and MSCs were seeded atop. For the 3D system, MSCs were encapsulated into PEGDA solution with UV sensitive initiator (irgacure 2959 and then polymerized using UV exposure. The cells were seeded for 2 days in both systems and then the conditioned media was transferred to hMVECs that were seeded on Matrigel. After 8 hours, tube formation was observed through microscopy.

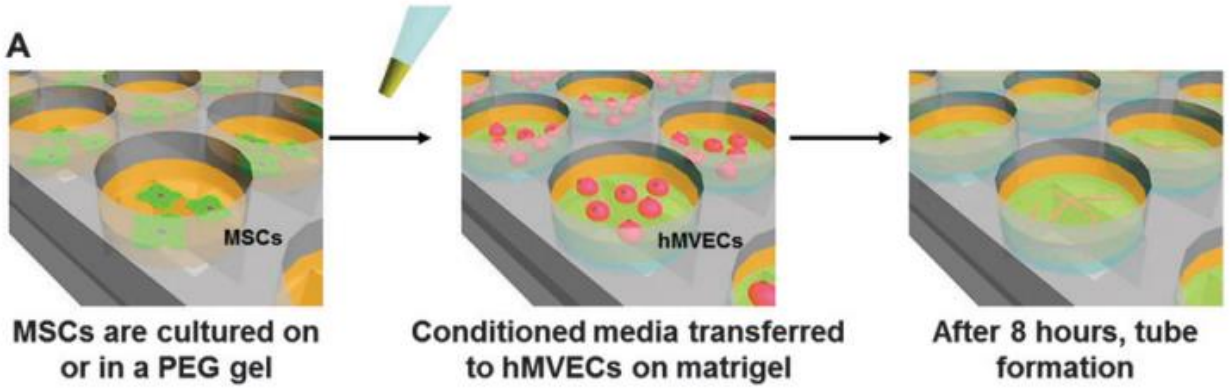

Figure 4. 1 – This schematic describes the procedure of taking cultured media from MSCs, then transferring the media from both dimensionalities, and then observing tube formation.[116]

4.2.2 – *PEG Encapsulation*

To compare the angiogenic potential of MSCs cultured on either 2D surface or a 3D architecture, PEG hydrogels were modified with diacrylate moieties. To attach the matrix proteins to the hydrogel, the proteins were functionalized with acrylate groups by reacting amines on the protein with NHS-acrylate. Then, a UV sensitive initiator (irgacure 2959) was used to introduce the matrix protein to the hydrogel network which was visually confirmed using fluorescent fibrinogen. Using data from previous work, fibronectin was used for as the matrix protein and the PEGDA hydrogels were modulated to have a stiffness of 40kPa.

This investigation required PEGDA, PEG conjugated with fibronectin, glass coverslips, TMSPM, , a photo mask, and a UV-crosslinker. When developing the platform to coculture the MSCs, we first had to determine how to incorporate different gel types onto one substrate.

The MSCs for both dimensionalities were cultured for two days, where the conditioned media was then collected and added to hMVECs seeded on 3D matrigel matrix. Shao et al. demonstrated a model system to study angiogenesis therefore we measure angiogeneic potential by seeding hMVECs on Matrigel matrix[117]. After eight hours since the conditioned media was introduced, tube formation of

the hMVECs was quantified and normalized to the tubulogensis seen from hMVECs when complete growth factor supplemented media was used.

After acknowledging that the conditioned media from the differing MSC cultures showed different tubulogenesis in hMVECs, the study progressed to investigate angiogenesis in a coculture system of encapsulated MSCs and hMVECs. Using state of the art fabrication tools and methods[49], gels were photopolymerized under UV exposure using a photomask to make distinct islands of MSCs encapsulated in PEGDA.

4.2.3 – *Hydrogel column fabrication*

The PEGDA coculture columns were fabricated onto glass coverslips that had a diameter of 18mm to fit into wells of a 12 well-plate. The glass coverslips were first cleaned by sonicating in ethanol for fifteen minutes, followed by sonication in deionized water for another fifteen minutes. The cleaned slides were then immersed in solution of 2% 3-(trimethoxysilyl)propyl methacrylate) (TMSPM) in ethanol with 0.3% glacial acetic acid for five minutes. Coverslips were then rinsed with ethanol, dried backside with a kimwipe, and then baked at 95 degC for one hour.

For the hydrogel preparation, PEGDA solutions of 30wt% and matrix proteins of acrylated fibronectin were prepared. To polymerize the PEGDA solution with UV exposure, the initiator 2-Hydroxy-4'-(2-hydroxyethoxy)-2-methylpropiophenone) was prepared at 10v/v% in ethanol and was protected from all light.

Once the PEGDA solutions, initiator, and matrix proteins are prepared, then preparation for cell encapsulation was taken. The MSCs were first incubated with cell tracker green in serum free media for 30 minutes at 5-10uM concentration. The cell tracker had to be resuspended in DMSO first before addition to the serum free media. For this experiment, we found that a 10mm plate of MSCs at around

80% confluency provided enough cells for four gels since most cells do not get encapsulated. While the cell tracker was incubating with the MSCs, the gel solutions were prepared for polymerization. For every 1mL of PEGDA solution, we added 5ul of initiator solution for a final concentration of 0.05% and added 50ug of acrylated fibronectin. This mixture was vortexed while wrapped in foil to avoid any exposure to light. After preparing this solution, the mask aligner was prepared by taping the appropriate mask to the glass plate. Careful examination was necessary to ensure the mask was facing the appropriate side for UV exposure. The bulb was then turned on to prepare for exposure after the cell tracker has incubated.

After the 30 minutes of incubation in cell tracker, the MSCs are trypsinized, and then transferred to 1.5ml centrifuge tubes. Cells were centrifuged at 300g for five minutes, and then resuspended in the PEGDA mixture. On a microscope glass slide prepared hydrophobically with Rain-X, 20ul of PEGDA mixture with cells was pipetted onto the slides, which was then covered with the prepared glass coverslips. This sandwich arrangement was then placed so the coverslip was below the glass slide with the ends of the microscope glass slide touching the mask at the desired pattern in the aligner.

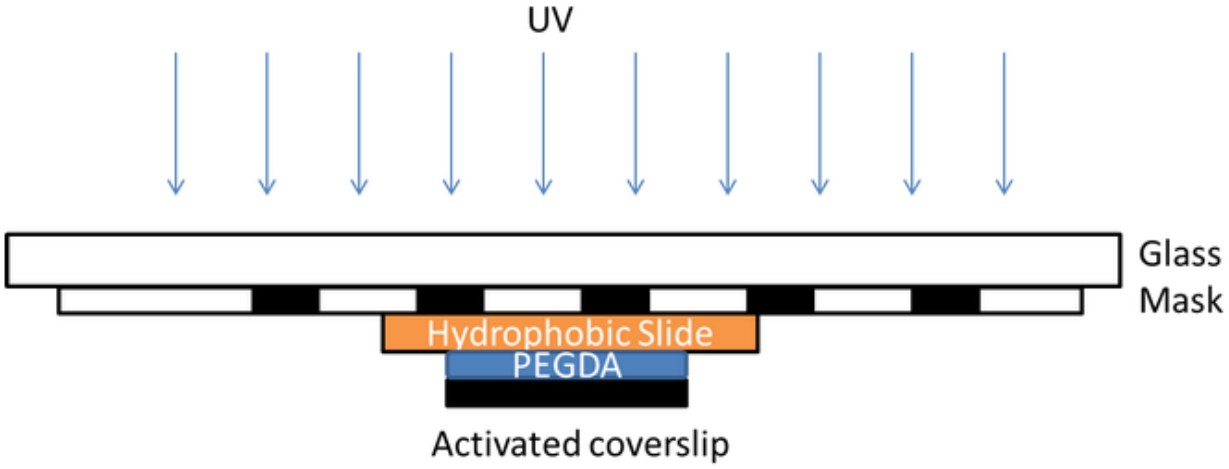

Figure 4. 2 – This schematic demonstrates the positioning of the hydrophobic glass slide that would anchor between the orifice on the mask aligner, which would then be exposed by the UV light polymerizing the PEGDA underneath it. The activated coverslip will remain attached to the hydrophobic slide through cohesive force of the gel solution.

The aligner was set for ten minutes and exposed the PEGDA for ten minutes. Afterwards, the mask was removed and the glass slides were placed on a stable surface. The coverslips were then removed from the hydrophobic glass slides so the PEGDA mixture with cells are on the activated coverslips. Using a forcep, the coverslips were held over a beaker with bleach and lightly washed off of unexposed PEGDA with deionized water. Under a microscope, we confirmed that the island patterns were properly exposed and that cells were encapsulated in the columns. Using another hydrophobic slide, we pipetted 50ul of Matrigel onto the surface which was followed by adding the coverslip of MSC islands facedown into it. These sandwiched slides were placed in the incubator for thirty minutes to polymerize the Matrigel.

While the Matrigel was polymerizing in the incubator, red cell tracker was added to hMVECs for 30 minutes in serum free EBM2 media without the growth factors. After the thirty minutes of solidifying, very carefully remove the coverslip with the Matrigel from the hydrophobic glass slide. Afterwards, we trypsinized the hMVECs and centrifuged at 300g for five minutes. A very important aspect was to ensure no residual cell tracker was left or else it ran the risk of entering the MSCs which would cause fluorescence from both cells in the red channel. The hMVECs were seeded at a density of 100,000 cells/gel in a 50:50 mixture of MSC and hMVEC media. From the initial seeding of the hMVEcs, the cells were checked every four hours and then fixed with 4% PFA at a timepoint between 8 and 24 hours. After fixation, the cells were mounted and then observed under fluorescent microscopy.

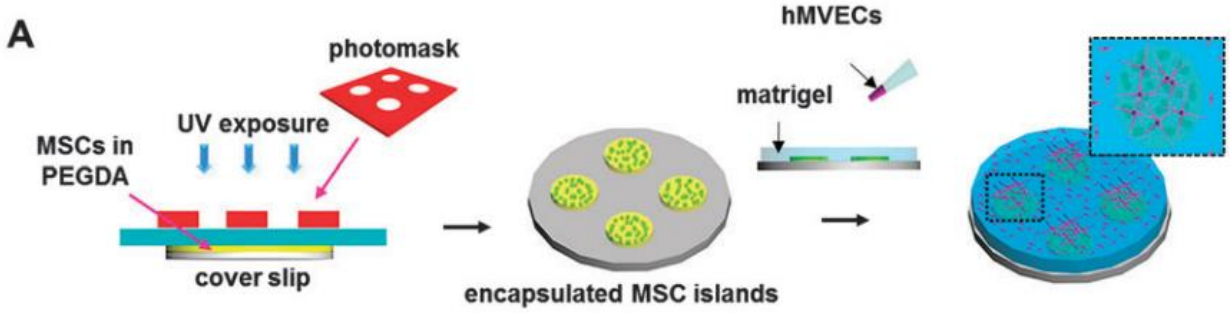

Figure 4. 3 – This schematic depicts the process of hydrogel fabrication with MSCs already encapsulated, to the culturing of hMVECs atop Matrigel.[116]

4.3 Results

Interested in observing role of dimensionality in culturing conditions on the secretome of MSCs, we either seeded MSCs on a 2D substrate or encapsulated them in 3D hydrogels systems and observed the angiogenic potential from its conditioned media. This experiment was conducted by observing the effects of the secretory profile from MSCs on the angiogenic potential of hMVECs. Influence of dimensionality on paracrine signaling is further investigated through our novel 3D spatially defined hydrogel co-culture system.

When observing the morphologies of the MSCs in the two different cultures, they were noticeably different. The cells on the 2D gel conditions demonstrated longer processes on the PEG hydrogel whereas the MSCs encapsulated did not demonstrate these spreading characteristics. When the MSCs were stained for actin, paxillin, and DAPI, it was also interesting to note that the fluorescence of paxillin was clearly evident with characteristics of focal adhesions for cells adherent to 2D substrates, but no evidence of focal complexes within encapsulated cells was apparent; actin was ubiquitously expressed through the cell body in cells of both conditions.

Comparing the effects of the conditioned media from both the 3D and 2D culture, there was a two fold increase in tubulogenesis in the 3D culture compared to the 2D culture. This can be visibly seen in the morphology of the tubes of the hMVECs when staining for actin. In fluorescent generated images, the vessels formed from encapsulated media were much longer and interconnected compared to the media from 2D structure. When comparing the results of tubulogenesis from serum free medium, to growth factor supplemented medium, to conditioned medium, there was least tubule formation observed in the serum free condition, with improved tubule formation in the growth factor

supplemented medium; however, the growth factor supplemented medium was only half the tubulogenesis seen in the conditioned medium (Figure 4.4).

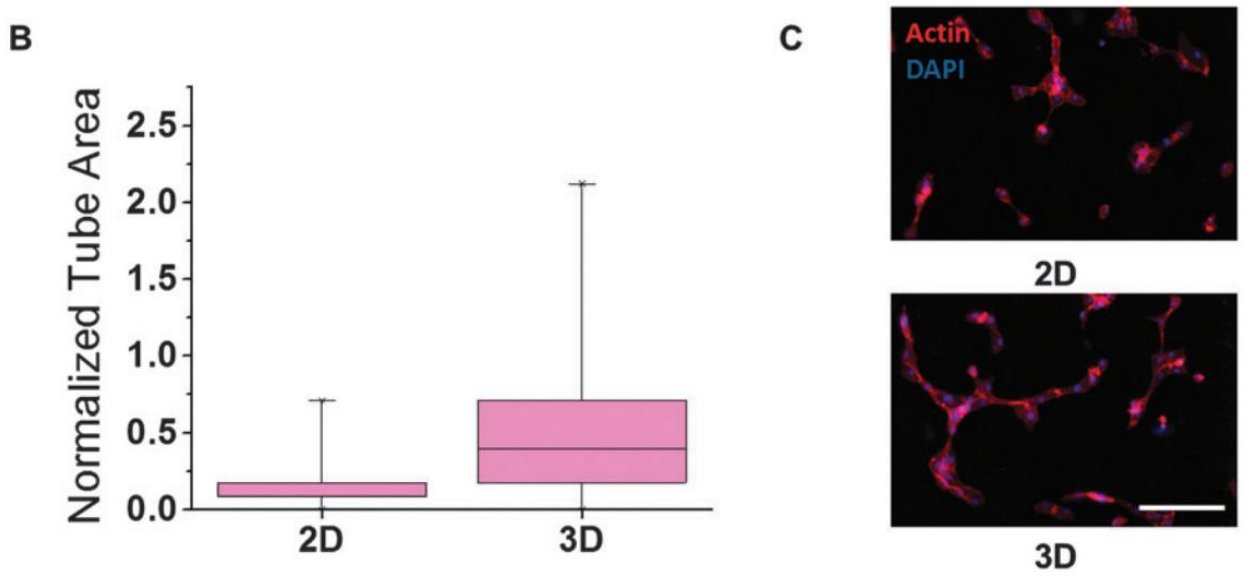

Figure 4. 4 – Quantitatively demonstrates the increased tubulogenesis measured from hMVECs cultured with conditioned media from 2D substrate vs 3D encapsulated environment in B. The difference in tubulogenesis can be observed from actin staining. (The scale bar is 200um.)[116]

The first experiment demonstrated that the dimensionality of MSC culture influenced the secretome that would alter the angiogenic potential of hMVECs that received conditions media. This experiment simulated paracrine signaling of MSCs with hMVECs through collected media, but further verification of paracrine signaling of MSCs was tested by observing angiogenesis of hMVECs in regions in contact with MSCs using spatially defined hydrogel columns verified by fluorescent beads in Figure 4.5. Once MSCs were encapsulated into islands of PEGDA columns and polymerized using UV exposure, Matrigel was placed on top, and then seeded with hMVECs atop the layer of Matrigel. After eight hours of culturing, angiogenic potential was observed where hMVECs exhibited tube formation on areas directly above the MSC islands, but hMVECs seeded outside the MSC regions showed very little tubulogenesis (Figure 4.5).

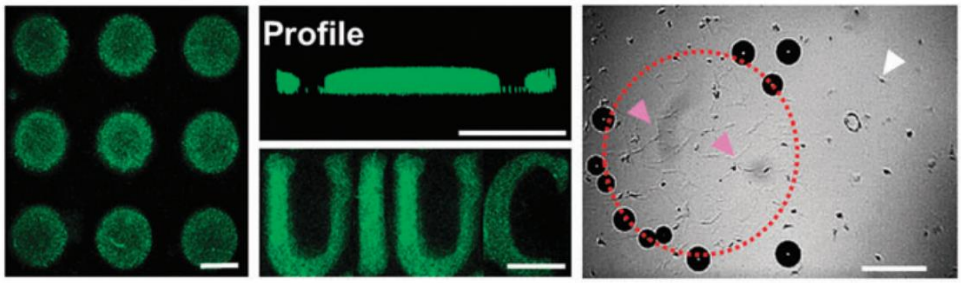

Figure 4. 5 – Spatial specificity of hydrogel columns are verified by embedded fluorescent beads. Specific patterns and shapes can also be attained seen by the UIUC logo and confocal imaging shows the profile of these columns. (The scale bar is 500um for the fluorescent images). Brightfield images also capture hMVECs at the surface of Matrigel that is directly above hydrogel column specified by the dotted line and tube formation shown by the pink arrow. (The scale bar is 1mm for the brightfield image). [116]

4.4 Discussion

Demonstrating the role of paracrine signaling between MSCs and hMVECs required designing a platform to spatially segregate both cell types. Since the first experiment showed that angiogenic potential was increased in 3 dimensional systems, spatially defined regions of encapsulated MSCs were required, but this proved difficult since encapsulating MSCs involved bulk mixing which would fail to spatially designate areas of encapsulated MSC. This hurdle was overcome by incorporating photolithography to spatially polymerize hydrogels with encapsulated MSCs which would later come in contact with hMVECs to study the effect of paracrine signaling. Developing this protocol required many steps of optimization from the determination of cells required for encapsulation, to the size of the islands, and exposure time. After each parameter was optimized, hydrogel columns with encapsulated cells were successfully made. The surrounding area was then filled with plain PEGDA with further UV exposure. Careful attention was paid to this fabrication method as fabrication methods required exposing encapsulated MSCs to non-physiologic conditions for at least twenty minutes for total exposure time and Matrigel gelation. Overall, the fabrication of this co-culture platform required optimization at every step, but is a robust system that can assay other paracrine signaling between cell types. We use angiogenesis as a model process to readily verify the paracrine

signaling reliance of MSCs and hMVECs, but this system can easily be adapted to model other cellular processes in heterotypic co-culture.

On a biomechanical level, the hydrogel columns allowed 3D cultures so the MSCs can experience full contact with the extracellular matrix whereas the cells seeded atop hydrogels can only physically sense the extracellular matrix on a planar level. The exposure of the ECM in 3D will influence downstream sensing modalities to guide the secretory profile of the cells and regulate behavior. In a related study comparing the cytokine secretion of 3D encapsulated cells to 2D cultured cells, there was a 35 fold increase between the environments which make the biological finding of this study reasonable[111]. Although it is important to acknowledge that other aspects of the microenvironment can also have an effect on the angiogenic potential by altering the secretome, dimensionality clearly plays a strong role. These results suggest that future designs of autologous scaffolds for tissue engineering should consider 3D culture environments to ensure an active secretome for optimal therapy.

Although we managed to investigate cellular behavior in 3-D, there are still many differences between our system and the in-vivo environment. Chief amongst them is cell's ability to remodel the matrix. In the next, and final, chapter we make an attempt and modifying PEG based hydrogels to include malleability to cell-based remodeling of the hydrogel.

Chapter 5

Synthesis of cell-responsive bis-aliphatic hydrazone hydrogels

As our last step towards improving in vitro model systems for tissue culture, we modify our PEG based system for cell responsiveness via modifying the crosslinking chemistry in this chapter.

5.1 Introduction

5.1.1 – *Importance to investigate cellular response to environment*

Once thought to serve as an inert scaffold for cells, investigators are finding the role of the ECM much more dynamic and crucial to cellular biology[118]. As the past two decades of research suggest the importance of ECM in cellular physiology, it is important to understand how the cell interacts with the ECM through remodeling[119]. During development of progenitor cells, regeneration of somatic cells, or even propagation of diseases, microenvironments are repurposed to cater to specific purposes of the cells. For example, it is well known that cancer cells alter the tumor microenvironment in different stages of cancer progression through invasive and metastatic alteration. By hijacking matrix metalloproteinases, cancer cells are able to degrade basement membrane and encourage angiogenesis to further supplement tumor growth[120]. In development of organs in vertebrae, branching morphogenesis is controlled tightly by function of proteinases that restructure the ECM. Even in skeletal development, the ECM undergoes a progression of remodeling to facilitate skeletal patterning, condensation, and differentiation to adult bone[118].

5.1.2 – *Utility of bis-aliphatic hydrazone bonds*

As scientists are garnering more interest in the microenvironment and its effect on cellular biology, it is important not only to recapture the microenvironment to simulate its effect on cellular systems, but it is also important to simulate how cellular systems respond to its environment and remodel it. Although the microenvironment comprises many components, it can be characterized to either a physical or biochemical role. There are currently a large number of assays available to investigate biochemical activity of cell behavior, but recapturing cellular remodeling on the microenvironment proves difficult on a biochemical level. Recently, investigators have started to simulate how cells can remodel the microenvironment physically by encapsulating cells in degradable hydrogels and observing cell growth progression. Although these methods exist to allow cells to degrade their microenvironment, it requires the use of proteinases to degrade specific cleavable bonds. An alternative to protein specific bonds is to utilize advances in mechanochemistry to use physically disruptable bonds such as disulfides linkages or bis-aliphatic hydrazone bonds. McKinnon et al. demonstrated that hydrazone bonds can be mechanically disrupted to produce an aldehyde and hydrazine[119]. In their study, they demonstrated that these hydrogels were capable of remodeling to neurite growth and extension suggesting that fabrication of such a gel may provide important biological insight into the development of other lineages. The unique application of novel mechanochemistry in the study of stem cell development prompts us to fabricate the robust bis-aliphatic hydrogels in hopes of simulating ECM remodeling.

5.2 Materials and methods

5.2.1 – Synthesis of functionalized PEG monomers

The synthesis of the bis-aliphatic PEG hydrogel required both monomers of PEG functionalized with aldehyde and one with hydrazine. For the oxidation of the alcohol group without using a toxic metal catalyst, swern oxidation was implemented. Oxalyl chloride was first dissolved in anhydrous DCM in a flask that was baked overnight, flame dried, then purged with argon. The flask containing the oxalyl chloride was then capped with a rubber stopper to prevent any further moisture from entering and then placed in a dry ice/acetone bath to reach a temperature of -78 deg C. In another flask that was baked overnight, flame dried, then purged with argon, anhydrous DMSO was added to the flask. The Schlenk line was connected to the flask with DMSO and then a cannula was connected from that flask to the flask with the oxalyl chloride with a syringe to release excess gas. The argon was then turned on to transfer DMSO dropwise to the oxalyl chloride with DCM. Afterwards, the cannula set up was dismantled and repeated with a new flame purged flask containing PEG dissolved in DCM. The PEG dissolved in DCM was then transferred dropwise onto the oxalyl chloride. After the PEG was allowed to react for 20 minutes, triethylamine was added dropwise allowing the reaction to warm to room temperature. The product was then precipitated with diethyl ether and was purified in dialysis tubes in DI water.

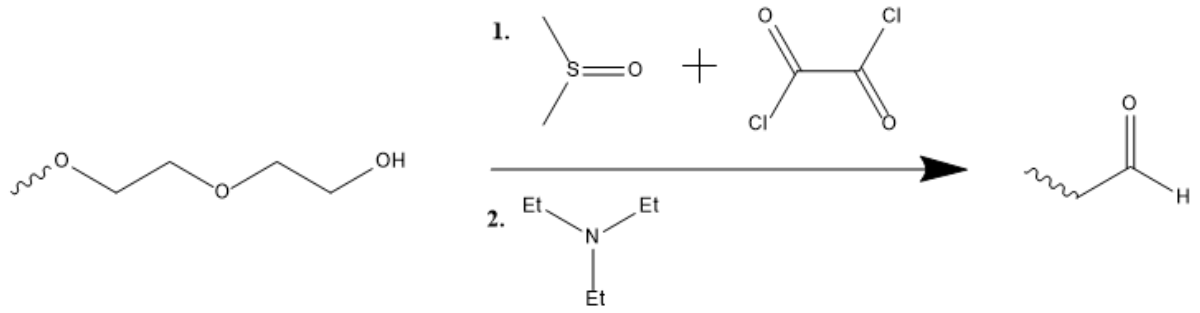

Figure 5. 1 – Depicts the conditions necessary for swern oxidation to oxidize the hydroxyl group from PEG without using a toxic metal.

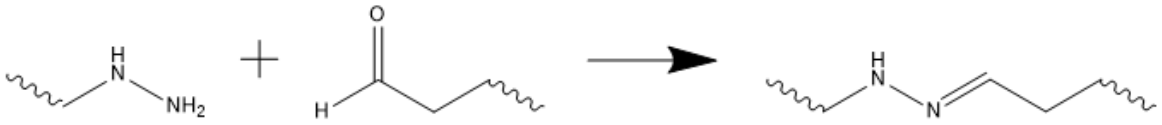

Figure 5. 2 – The hydrazine functional group nucleophilcally attacks the carbonyl carbon of the aldehyde through imine formation releasing a water.

5.2.2 – *Synthesis of bis-aliphatic hydrazone hydrogels*

The hydrazone hydrogels were synthesized by allowing PEG-Ald and PEG-Hz dissolved in buffered saline solution to react at room temperature. Using a 30 wt% solution of PEG-Hz and 15 wt% of PEG-Ald, the solutions were combined stoichiometrically in microcentrifuge tubes. They were then pipetted onto hydrophobically treated glass slides and then sandwiched under glass coverslips with aldehyde functionality to adhere onto its surface. After gelating on the glass slide, the coverslips were removed with forceps.

5.3 Results

The synthesis of the bis-aliphatic hydrazone hydrogels took many attempts due to difficulty of oxidizing the hydroxyl group on PEG to an aldehyde. In the first attempt of swern oxidation, addition of the triethylamine turned the reaction flask a bright lime yellow which later turned into a dark musky brown during the 20 minute reaction timeframe. When precipitating, there was a powder that formed

amidst a layer of darker brown solution which also had a staunch smell suggesting the byproduct dimethylsulfide was formed. In the ether, there were two distinctive layers and each successive separation did not separate the dark brown substance (Figure 5.3). In attempt to further separate the layers, the mixture was left in ether over night before filtering once more. There was a thick layer of brown byproduct unremovable from the PEG from the filtering, but was placed into dialysis bags.

Figure 5. 3 – First attempt at oxidizing PEG led to precipitate and dark brown by-product.

The reaction mixture that started off dark brown in the dialysis tubes started to dilute in the tanks of DI water that held approximately eight liters with water replaced daily (Figure 5.4). After two weeks of dialysis, the remaining solution was filtered once more with ether, and then lyophilized. The lyophilized PEG-Ald was mixed 15% v/v in water and PEG-Hz was mixed 30% v/v in water. On a glass coverslip that was treated with APTS and glutaraldehyde, the PEG mixture was placed on a hydrophobic microscope slide and then allowed

to gelate for time points at increments of ten minutes up to an hour. Under each coverslip, a viscous mixture remained, but no gel was formed.

Figure 5. 4 – Dialysis tubes containing the first attempt of PEG oxidation shows dilution in byproduct as they diffuse into pure DI.

The swern oxidation was repeated a second time with fresh DMSO to ensure no moisture was present. After adding the triethylamine and allowing the reaction to room temperature, it was observed the reaction flask was very light brown. After the final product was dissolved in ether, the mixture appeared white and it was left overnight.

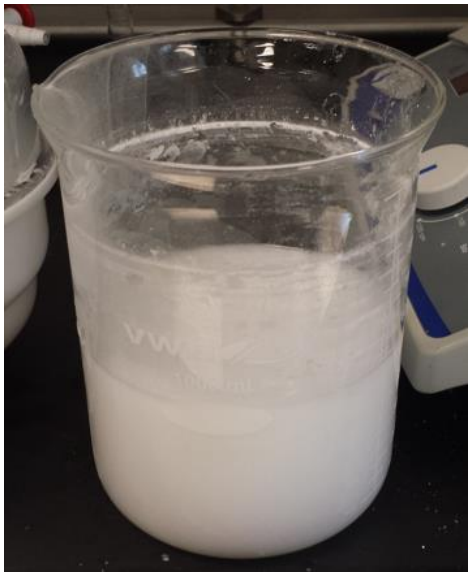

Figure 5. 5 – The reaction mixture after the second swern oxidation suggests there are less acid chloride byproducts from the lack of brown color.

Similar to the first attempt to make gels, 15% v/v PEG-Ald was dissolved in water and 30% v/v PEG-Hz. Coverslips treated with APTS and glutaraldehyde was prepared along hydrophobic glass slides. In micro-centrifuge tubes, 33uL of each PEG was allowed to mix in tube for 5 minutes before pipetted onto the slide and covered. In the next trial, the same amount was mixed in a micro-centrifuge tube, but for three minutes before pipetting onto a hydrophobically treated microscope slide. Lastly, 45ml of each PEG solution was mixed in a centrifuge tube and vortexed for thirty seconds, and then allowed to rest in the tube for a minute before pipetting onto the slide. In each trial condition, mixtures under separate coverslips were allowed to react and were checked for gelation periodically. In the first trial condition, a viscous mixture resulted, but no gel was formed in time points of one, three, five, ten and every ten minutes afterwards until an hour. In the second trial, gelation was observed for time points after three minutes and beyond. Similarly, the third trial also exhibited gelation with wavy gels formed at two minutes and beyond.

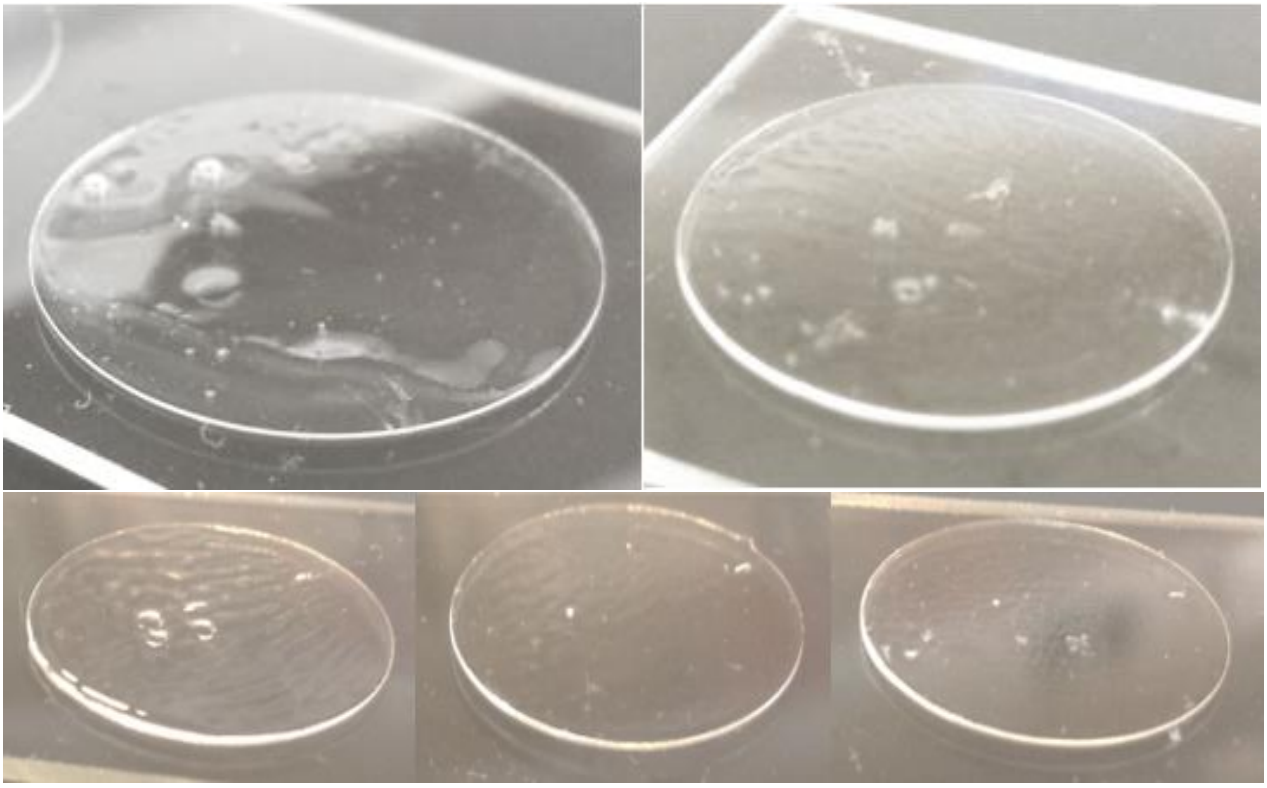

Figure 5. 6 – The top row are the gels that formed under trial two with three minutes and five minutes results shown respectively. The bottom row depicts the gels that were formed in trial three. From left to right, the gels were formed at two, three, and nine minutes demonstrating the progression of gel topology.

We realized that the gels that formed had very small volumes suggesting there was little swelling occurring in these gels. Placing the gels in wells in a 12 well plate, the gels remained thin and retained the rough surface from before. The gels were still attached to the coverslips suggesting that the glutaraldehyde was sufficient to conjugate the hydrazine from the gel onto the surface. Since the best results for gelating occurred in the third trial, we then tried vortexing the gel to induce physical mixing, and then left it in the micro-centrifuge tube for 4.5, 7.5 and 8 minutes. Afterwards, the gel mixture was pipetted onto the microscope glass slide and left to react for 5, 10, and 15 minutes. In the first trial, a gel did not form at 5 minutes, but a thin gel with ridges was made at 10 minutes and slightly better developed gel was formed at 15 minutes. In the second trial, there were similar results with no gel forming at 5 minutes, but a thin gel forming at 10 and 15 minutes. The gels in the second trial; however, showed less ridges with no remaining mixture of PEG. By the time the PEG mixture was

allowed to react in the micro-centrifuge tube for 8 minutes, it gelated preventing any further pipetting onto the microscope glass slide.

The pipette volume may have impacted the ability for gels to form physical bonds, but maybe not given enough room to form sufficient hydrazone bonds. This prompted us to experiment with different amounts of pipetting volume. Starting from a pipetting volume from 10 uL and increasing it by 10 uL until 60uL, we observed that gel thickness increased from 20 to 40uL, but the gels at 50uL and 60uL had similar thickness with residual water around the gel.

Figure 5. 7 – Increasing the pipette volume improved gel thickness from 20-40uL shown in the left image, but further addition of gel mixture left liquid residue in the body of the coverslip shown by the 60uL droplet in the image on the right

5.4 Discussion

The first synthesis of PEG-aldehyde proved to be challenging, but provided direction for attempting a swern oxidation. During the first swern oxidation, dark brown precipitate was formed suggesting it was the formation of acid chloride byproducts[121]. Following stoichiometric ratios given in the protocol from McKinnon et al.[119], the amount of oxalyl chloride may have been excessive for the 4-arm PEG that we used prompting us to use half the stoichiometric amount of reagents given an amount of PEG.

After the long duration of dialysis, it was determined that the created product did not gelate with PEG-hydrazine suggesting the reaction occurred to create the sulfonium intermediate.

Our second attempt of swern oxidation produced a PEG-ald that gelated with PEG-Hz, but with limited success. The lack of brown precipitate in the reaction flask during swern oxidation also suggested that conditions allowed for successful oxidation with minimal byproducts formed. It was interesting to note that the hydrazone PEG gels formed faster than PEGDA hydrogels. Allowed to hydrate in water in well plates, the hydrazone gels didn't swell like the PEGDA hydrogels and it retained the ridges on its surface even after hydrating. Furthermore, even with increased pipetting volume of the gel mixture, the thickness of each hydrazone gel remained much thinner than PEGDA gels despite using volumes greater than the PEGDA gels.

The gelation of the suspected PEG-aldehyde suggests an aldehyde was indeed oxidized from an alcohol since the amine from the hydrazine would then be able to form an imine with the aldehyde. Further chemical analysis on the bonding of the gel must be made to ascertain the extent of hydrazone bond formation. The small variations of trials to create a swelling gel suggests that physical gelling indeed did occur, most likely caused by the weight of the coverslip forcing the multiarm PEG to interact intimately with the linear PEG intercalating between with chemical bonding formed when possible. This hypothesis can be further supported from gels that were formed in the micro-centrifuge tubes. When the micro-centrifuge tubes had PEG-ald and PEG-Hz mixed in, vortexed, then left alone to gel, the hydrogel remained even when water was added to the centrifuge tube. Even after leaving water in overnight, the gel remained when the water in the tube was poured out suggesting that when no volumetric constraint was applied, sufficient chemical bonding was formed to prevent dissociation unlike the gels formed under coverslip where PEG chains would eventually float freely when swollen with water since there wasn't sufficient hydrazone bond formation.

The third batch of PEG-aldehyde formed from swern oxidation was less successful than the second with no gelling and only viscous liquid formation after mixed with PEG-hydrazine. Furthermore, there was a peak at $\delta = 11.8$ suggesting a hydrogen from a carboxylic acid which may have formed from possible moisture reacting with oxalyl chloride which may have then reacted with the hydroxyl. This would also explain the inability to form gels even though the reaction mixture seemed to contain little acid chloride byproduct based on the lack of brown precipitate.

5.4.1 – *Future Works*

The utility of exploring mechano-sensitive polymer networks has broad biological implications when investigating the response a cell may incur onto its environment through remodeling, particularly physical remodeling. Our study suggests that forming bis-aliphatic hydrazone hydrogels is only half the trouble, but optimizing the gel in a platform to study cell remodeling may prove more difficult. Although McKinnon et al. demonstrated neurite extension using this gel network, we wish to utilize this gel in a wide variety of biomechanic applications to study specific cellular processes that can remodel the microenvironment such as cellular migration and remodeling to adopt new morphologies during lineage specification. Granted that cells exist in three dimensional environments, investigating many of these physical and mechanical processes are much more easily studied in a two-dimensional platform prompting us to develop a method to form these bis-aliphatic hydrazone hydrogels on coverslips with improved chemical bonding to allow hydrogels to swell in cell medium without dissolving.

Understanding the morphological remodeling that occurs in differentiating stem cells is of interest to biologists, and dynamic hydrogel materials may provide a platform to explore this class of mechanochemical signaling. It is well observed the different morphologies that may occur in different

embryonic days of developing organs or tissue systems, but not studied before is the physical remodeling that organogenesis may exert to allow for such processes. Specifically, it would be very exciting to investigate the physical remodeling that stem cells exert during differentiation, progenitor-like cells during transdifferentiation, and somatic cells during direct reprogramming. Insight into the physical remodeling that these cells undergo will give vital understanding of mechanisms that can bolster the efficiency of the lineage specification and provide further methods to alter scaffolding materials to improve regeneration in tissue engineering applications.

Chapter 6

Conclusions

Hydrogel platforms provide a robust means to investigate the intricate cross talk between cells and their mechanical microenvironment. As dynamic systems that retain large water content with versatile functionality, mimicry of tissue environment provides deeper understanding of cell physiology and provides a stepping stone for engineering new materials. From the fabrication of hydrogels to successful patterning, we demonstrate that they can assay biological responses not only from its mechanical environment, but also in conjunction with its biochemical environment. We explore both 2D and 3D hydrogel models as based on the need of the experiment. As discussed, 2D systems are more robust platforms with simpler experimental setup and readout; however, 3D systems provide more accurate biomimetic information bridging the synthetic simulation gap. This has been demonstrated by our study exploring the mechanical influence on a cells secretome. Culturing MSCs in different dimensionalities altered their paracrine profile verified by increased angiogenic potential of hMVECs. This is further shown through spatially defined co-culture hydrogel systems where physiological mimicry serve to increase cellular functionality. As stem cell attract many scientists and physicians as compatible and regenerative therapies with maximum functionality, exploring strategies for lineage specification can repopulate diseased/damaged cells and provide natural healing. Specifically interested in optimizing neurogenic specification through a combinatorial approach of lipid derived molecules and cell mechanics, we demonstrate that cell behavior is modulated from both environmental factors highlighting the complex interplay that can be manipulated for optimized fate commitment. From simple hydrogel fabrication to complex environments incorporating many environmental cues, engineering hydrogel materials is a promising platform to elucidate unknown pathways and push the field of biomaterials and medicine.

References

1. Buwalda, S. J. *et al.* Hydrogels in a historical perspective: From simple networks to smart materials. *J. Control. Release* **190,** 254–273 (2014).

2. Kope??ek, J. Hydrogel biomaterials: A smart future? *Biomaterials* **28,** 5185–5192 (2007).

3. Kopecek, J. Polymer chemistry: swell gels. *Nature* **417,** 388–389, 391 (2002).

4. White, E. M., Yatvin, J., Grubbs, J. B., Bilbrey, J. A. & Locklin, J. Advances in smart materials: Stimuli-responsive hydrogel thin films. *J. Polym. Sci. Part B Polym. Phys.* **51,** 1084–1099 (2013).

5. Koetting, M. C., Peters, J. T., Steichen, S. D. & Peppas, N. A. Stimulus-responsive hydrogels: Theory, modern advances, and applications. *Mater. Sci. Eng. R Reports* **93,** 1–49 (2015).

6. Döring, A., Birnbaum, W. & Kuckling, D. Responsive hydrogels--structurally and dimensionally optimized smart frameworks for applications in catalysis, micro-system technology and material science. *Chem. Soc. Rev.* **42,** 7391–420 (2013).

7. Ahmed, E. M. Hydrogel: Preparation, characterization, and applications: A review. *J. Adv. Res.* **6,** 105–121 (2015).

8. Shimada, N., Kidoaki, S. & Maruyama, A. Smart hydrogels exhibiting UCST-type volume changes under physiologically relevant conditions. *RSC Adv.* **4,** 52346–52348 (2014).

9. Xu, X., Jha, A, Harrington, DA., Farach-Carson, M. Hyaluronic Acid - Based Hydrogel: from a Natural Polysaccharide to Complex Networks. *Soft Matter* **8,** 3280–3294 (2012).

10. Hesse, E. *et al.* Collagen type I hydrogel allows migration, proliferation and osteogenic differentiation of rat bone marrow stromal cells. *J. Biomed. Mater. Res.* **94,** 442–449 (2011).

11. Janmey, P. A., Winer, J. P. & Weisel, J. W. Fibrin gels and their clinical and bioengineering applications. *J. R. Soc. Interface* **6,** 1–10 (2009).

12. Rowley, J. A., Madlambayan, G. & Mooney, D. J. Alginate hydrogels as synthetic extracellular matrix materials. *Biomaterials* **20,** 45–53 (1999).

13. Bhattarai, N., Gunn, J. & Zhang, M. Chitosan-based hydrogels for controlled, localized drug delivery. *Adv. Drug Deliv. Rev.* **62,** 83–99 (2010).

14. Kandow, C. E., Georges, P. C., Janmey, P. A. & Beningo, K. A. Polyacrylamide Hydrogels for Cell Mechanics: Steps Toward Optimization and Alternative Uses. *Methods Cell Biol.* **83,** 29–46 (2007).

15. Raeber, G. P., Lutolf, M. P. & Hubbell, J. A. Molecularly Engineered PEG Hydrogels: A Novel Model System for Proteolytically Mediated Cell Migration. *Biophys. J.* **89,** 1374–1388 (2005).

16. Jiang, S., Liu, S. & Feng, W. PVA hydrogel properties for biomedical application. *J. Mech. Behav. Biomed. Mater.* **4,** 1228–1233 (2011).

17. Gatzeva-topalova, P. Z., Warner, L. R., Pardi, A. & Carlos, M. NIH Public Access. **18,** 1492–1501 (2011).

18. Burdick, J. A., Chung, C., Jia, X., Randolph, M. A. & Langer, R. NIH Public Access. **6,** 386–391 (2009).

19. Bordi, F., Paradossi, G., Rinaldi, C. & Ruzicka, B. Chemical and physical hydrogels: Two casesystems studied by quasi elastic light scattering. *Phys. A Stat. Mech. its Appl.* **304,** 119–128 (2002).

20. Begam, T., Nagpal, A. K. & Singhal, R. A Comparative Study of Swelling Properties of Hydrogels Based on Poly (acrylamide- co -methyl methacrylate) Containing Physical and Chemical Crosslinks. *J. Appl. Polym. Sci.* **89,** 779–786 (2003).

21. Yahia, L. H., Chirani, N., Gritsch, L., Motta, F. L. & Natta, C. G. History and Applications of Hydrogels. *iMedPub Journals* **4,** 1–23 (2015).

22. Ishikiriyama, K., Todoki, M., Kobayashi, T. & Tanzawa, H. Pore Size Distribution Measurements of Poly(methyl methacrylate) Hydrogel Membranes for Artificial Kidneys Using Differential Scanning Calorimetry. *J. Colloid Interface Sci.* **173,** 419–428 (1995).

23. Annabi, N. *et al.* Controlling the porosity and microarchitecture of hydrogels for tissue engineering. *Tissue Eng. Part B. Rev.* **16,** 371–383 (2010).

24. Cal??, E. & Khutoryanskiy, V. V. Biomedical applications of hydrogels: A review of patents and commercial products. *Eur. Polym. J.* **65,** 252–267 (2015).

25. Wang, X., He, J., Wang, Y. & Cui, F.-Z. Hyaluronic acid-based scaffold for central neural tissue engineering. *Interface Focus* **2,** 278–291 (2012).

26. Dmochowski, R. R. & Appell, R. A. Injectable agents in the treatment of stress urinary incontinence in women: where are we now? *Urology* **56,** 32–40 (2000).

27. Tian, Y. *et al.* A Peptide-Based Nano fi brous Hydrogel as a Promising DNA Nanovector for Optimizing the E ffi cacy of HIV Vaccine. 10–16 (2014).

28. Tsao, C. T. *et al.* Thermoreversible poly(ethylene glycol)-g-chitosan hydrogel as a therapeutic T lymphocyte depot for localized glioblastoma immunotherapy. *Biomacromolecules* **15,** 2656–2662 (2014).

29. Engler, A. J., Sen, S., Sweeney, H. L. & Discher, D. E. Matrix Elasticity Directs Stem Cell Lineage Specification. *Cell* **126,** 677–689 (2006).

30. Lee, J., Abdeen, A. A., Zhang, D. & Kilian, K. A. Directing stem cell fate on hydrogel substrates by controlling cell geometry, matrix mechanics and adhesion ligand composition. *Biomaterials* **34,** 8140–8148 (2013).

31. Tibbitt, M. W. & Anseth, K. S. Hydrogels as extracellular matrix mimics for 3D cell culture. *Biotechnol. Bioeng.* **103,** 655–663 (2009).

32. Trappmann, B. & Chen, C. S. Perspective. **24,** 948–953 (2014).

33. Wen, J. H. *et al.* Interplay of matrix stiffness and protein tethering in stem cell differentiation. *Nat. Mater.* **advance on,** 1–21 (2014).

34. Baker, B. M. & Chen, C. S. Deconstructing the third dimension - how 3D culture microenvironments alter cellular cues. *J. Cell Sci.* **125,** 3015–3024 (2012).

35. Mseka, T., Bamburg, J. R. & Cramer, L. P. ADF/cofilin family proteins control formation of oriented actin-filament bundles in the cell body to trigger fibroblast polarization. *J. Cell Sci.* **120,** 4332–44 (2007).

36. Tse, J. R. & Engler, A. J. Preparation of hydrogel substrates with tunable mechanical properties. *Curr. Protoc. Cell Biol.* 1–16 (2010). doi:10.1002/0471143030.cb1016s47

37. Aydin, D. *et al.* Polymeric substrates with tunable elasticity and nanoscopically controlled biomolecule

presentation. *Langmuir* **26,** 15472–15480 (2010).

38. Wang, J. H. C. & Thampatty, B. P. An introductory review of cell mechanobiology. *Biomech. Model. Mechanobiol.* **5,** 1–16 (2006).

39. Ruiz, S. A. & Chen, C. S. Emergence of patterned stem cell differentiation within multicellular structures. *Stem Cells* **26,** 2921–2927 (2008).

40. Hartman, M. A. & Spudich, J. A. The myosin superfamily at a glance. *J. Cell Sci.* **125,** 1627–1632 (2012).

41. Wang, N., Butler, J. P. P. & Ingber, D. E. E. Mechanotransduction across the cell surface and through the cytoskeleton. *Science* **260,** 1124–1127 (1993).

42. Huijing, P. A. & Jaspers, R. T. Adaptation of muscle size and myofascial force transmission: A review and some new experimental results. *Scand. J. Med. Sci. Sport.* **15,** 349–380 (2005).

43. Geiger, B., Bershadsky, A., Pankov, R., Yamada, K. M. & Correspondence, B. G. Transmembrane extracellular matrix– cytoskeleton crosstalk. *Nat. Rev. Mol. Cell Biol.* **2,** 793–805 (2001).

44. Choquet, D., Felsenfeld, D. P. & Sheetz, M. P. Extracellular matrix rigidity causes strengthening of integrin-cytoskeleton linkages. *Cell* **88,** 39–48 (1997).

45. Maniotis, A. J., Chen, C. S. & Ingber, D. E. Demonstration of mechanical connections between integrins, cytoskeletal filaments, and nucleoplasm that stabilize nuclear structure. *Proc. Natl. Acad. Sci. U. S. A.* **94,** 849–54 (1997).

46. Hu, S., Chen, J., Butler, J. P. & Wang, N. Prestress mediates force propagation into the nucleus. *Biochem. Biophys. Res. Commun.* **329,** 423–428 (2005).

47. Parker, K. K. & Ingber, D. E. Extracellular matrix, mechanotransduction and structural hierarchies in heart tissue engineering. *Philos. Trans. R. Soc. Lond. B. Biol. Sci.* **362,** 1267–79 (2007).

48. Ingber, D. E. Cellular mechanotransduction: putting all the pieces together again. *FASEB J.* **20,** 27 (2006).

49. Li, Y. & Kilian, K. A. Bridging the Gap: From 2D Cell Culture to 3D Microengineered Extracellular Matrices. *Adv. Healthc. Mater.* **4,** 2780–2796 (2015).

50. Cosson, S. & Lutolf, M. P. Microfluidic patterning of protein gradients on biomimetic hydrogel substrates. *Methods Cell Biol.* **121,** 91–102 (2014).

51. Kilian, K. A., Bugarija, B., Lahn, B. T. & Mrksich, M. Geometric cues for directing the differentiation of mesenchymal stem cells. *Proc. Natl. Acad. Sci. U. S. A.* **107,** 4872–7 (2010).

52. McBeath, R., Pirone, D. M., Nelson, C. M., Bhadriraju, K. & Chen, C. S. Cell shape, cytoskeletal tension, and RhoA regulate stem cell lineage commitment. *Dev. Cell* **6,** 483–495 (2004).

53. Desai, R. a, Khan, M. K., Gopal, S. B. & Chen, C. S. Subcellular spatial segregation of integrin subtypes by patterned multicomponent surfaces. *Integr. Biol. (Camb).* **3,** 560–7 (2011).

54. Majumdar, M. K. *et al.* Characterization and functionality of cell surface molecules on human mesenchymal stem cells. *J. Biomed. Sci.* **10,** 228–241 (2003).

55. Wozniak, M. A., Modzelewska, K., Kwong, L. & Keely, P. J. Focal adhesion regulation of cell behavior. *Biochim. Biophys. Acta* **1692,** 103–19 (2004).

56. Kilian, K. A. & Mrksich, M. Directing stem cell fate by controlling the affinity and density of ligand-receptor interactions at the biomaterials interface. *Angew. Chemie - Int. Ed.* **51,** 4891–4895 (2012).

57. Hunkeler, D. Mechanism and kinetics of the persulfate-initiated polymerization of acrylamide. *Macromolecules* **24,** 2160–2171 (1991).

58. Abdeen, A. A., Weiss, J. B., Lee, J. & Kilian, K. A. Matrix composition and mechanics direct proangiogenic signaling from mesenchymal stem cells. *Tissue Eng. Part A* **20,** 2737–45 (2014).

59. Lee, J., Abdeen, A. A., Huang, T. H. & Kilian, K. A. Controlling cell geometry on substrates of variable stiffness can tune the degree of osteogenesis in human mesenchymal stem cells. *J. Mech. Behav. Biomed. Mater.* **38,** 209–218 (2014).

60. Gumbiner, B. M. Cell adhesion: The molecular basis of tissue architecture and morphogenesis. *Cell* **84,** 345–357 (1996).

61. Sanjana, N. E. & Fuller, S. B. A fast flexible ink-jet printing method for patterning dissociated neurons in culture. *J. Neurosci. Methods* **136,** 151–163 (2004).

62. Magome, N. & Agladze, K. Patterning and excitability control in cardiomyocyte tissue culture. *Phys. D Nonlinear Phenom.* **239,** 1560–1566 (2010).

63. Bazinet, R. P. & Layé, S. Polyunsaturated fatty acids and their metabolites in brain function and disease. *Nat. Rev. Neurosci.* **15,** 771–785 (2014).

64. Arbabi, L., Baharuldin, M. T. H., Moklas, M. A. M., Fakurazi, S. & Muhammad, S. I. Antidepressant-like effects of omega-3 fatty acids in postpartum model of depression in rats. *Behav. Brain Res.* **271,** 65–71 (2014).

65. Zhang, M. *et al.* Omega-3 fatty acids protect the brain against ischemic injury by activating Nrf2 and upregulating heme oxygenase 1. *J. Neurosci.* **34,** 1903–15 (2014).

66. Li, P. *et al.* Epoxyeicosatrienoic acids enhance embryonic haematopoiesis and adult marrow engraftment. *Nature* **523,** 468–471 (2015).

67. Kim, D. H. *et al.* Epoxyeicosatrienoic acid agonist regulates human mesenchymal stem cell-derived adipocytes through activation of HO-1-pAKT signaling and a decrease in PPARγ. *Stem Cells Dev.* **19,** 1863–73 (2010).

68. Fomby, P. & Cherlin, A. J. NIH Public Access. **72,** 181–204 (2011).

69. Kim, H. Y., Spector, A. A. & Xiong, Z. M. A synaptogenic amide N-docosahexaenoylethanolamide promotes hippocampal development. *Prostaglandins Other Lipid Mediat.* **96,** 114–120 (2011).

70. Farmer, S. R. Regulation of PPARgamma activity during adipogenesis. *Int. J. Obes. (Lond).* **29 Suppl 1,** S13–S16 (2005).

71. Berger, J. & Moller, D. E. T m a ppar. (2002).

72. Takahashi, K. *et al.* Induction of Pluripotent Stem Cells from Adult Human Fibroblasts by Defined Factors. *Cell* **131,** 861–872 (2007).

73. Ma, T., Xie, M., Laurent, T. & Ding, S. Progress in the reprogramming of somatic cells. *Circ. Res.* **112,** 562–574 (2013).

74. Ben-David, U. & Benvenisty, N. The tumorigenicity of human embryonic and induced pluripotent stem cells. *Nat. Rev. Cancer* **11,** 268–77 (2011).

75. Li, X. *et al.* Small-Molecule-Driven Direct Reprogramming of Mouse Fibroblasts into Functional Neurons. *Cell Stem Cell* **17,** 195–203 (2015).

76. Xu, J., Du, Y. & Deng, H. Direct lineage reprogramming: Strategies, mechanisms, and applications.

Cell Stem Cell **16,** 119–134 (2015).

77. Cheng, L. *et al.* Generation of neural progenitor cells by chemical cocktails and hypoxia. *Cell Res.* **24,** 665–679 (2014).

78. Lee, J., Abdeen, A. A. & Kilian, K. A. Rewiring mesenchymal stem cell lineage specification by switching the biophysical microenvironment. *Sci. Rep.* **4,** 5188 (2014).

79. Dokmanovic, M., Clarke, C. & Marks, P. a. Histone deacetylase inhibitors: overview and perspectives. *Mol. Cancer Res.* **5,** 981–9 (2007).

80. Burgess, D. J. Stem cells: Histone deacetylase inhibitors for stem cell boost. *Nat. Rev. Genet.* **15,** 364 (2014).

81. Chaurasia, P., Gajzer, D. C., Schaniel, C., Souza, S. D. & Hoffman, R. Epigenetic reprogramming induces the expansion of cord blood stem cells. *J. Clin. Invest.* **124,** 2378–2395 (2014).

82. Kim, H. J., Leeds, P. & Chuang, D. M. The HDAC inhibitor, sodium butyrate, stimulates neurogenesis in the ischemic brain. *J. Neurochem.* **110,** 1226–1240 (2009).

83. George, S. *et al.* Impact of trichostatin A and sodium valproate treatment on post-stroke neurogenesis and behavioral outcomes in immature mice. *Front. Cell. Neurosci.* **7,** 123 (2013).

84. Shakèd, M. *et al.* Histone deacetylases control neurogenesis in embryonic brain by inhibition of BMP2/4 signaling. *PLoS One* **3,** (2008).

85. Yoo, D. Y. *et al.* Synergistic effects of sodium butyrate, a histone deacetylase inhibitor, on increase of neurogenesis induced by pyridoxine and increase of neural proliferation in the mouse dentate gyrus. *Neurochem. Res.* **36,** 1850–1857 (2011).

86. Iliff, J. J. *et al.* Epoxyeicosanoid signaling in CNS function and disease. *Prostaglandins Other Lipid Mediat.* **91,** 68–84 (2010).

87. Sundararajan, S., Jiang, Q., Heneka, M. & Landreth, G. PPARgamma as a therapeutic target in central nervous system diseases. *Neurochem Int* **49,** 136–144 (2006).

88. Wang, L. *et al.* 14,15-EET promotes mitochondrial biogenesis and protects cortical neurons against oxygen/glucose deprivation-induced apoptosis. *Biochem. Biophys. Res. Commun.* **450,** 604–609 (2014).

89. Chen, J. K., Falck, J. R., Reddy, K. M., Capdevila, J. & Harris, R. C. Epoxyeicosatrienoic acids and their sulfonimide derivatives stimulate tyrosine phosphorylation and induce mitogenesis in renal epithelial cells. *J. Biol. Chem.* **273,** 29254–29261 (1998).

90. Yuan, L. *et al.* 14,15-epoxyeicosatrienoic acid promotes production of BDNF from astrocytes and exerts neuroprotective effects during ischemic injury. *Neuropathol. Appl. Neurobiol.* n/a–n/a (2015). doi:10.1111/nan.12291

91. Shao, Z. *et al.* Cytochrome P450 2C8 ω3-long-chain polyunsaturated fatty acid metabolites increase mouse retinal pathologic neovascularization-brief report. *Arterioscler. Thromb. Vasc. Biol.* **34,** 581–586 (2014).

92. Font, M. A., Arboix, A. & Krupinski, J. Angiogenesis, neurogenesis and neuroplasticity in ischemic stroke. *Curr. Cardiol. Rev.* **6,** 238–44 (2010).

93. Xiong, Y., Mahmood, A. & Chopp, M. Angiogenesis, neurogenesis and brain recovery of function following injury. *Curr. Opin. Investig. Drugs* **11,** 298–308 (2010).

94. Arnold, C. *et al.* Arachidonic acid-metabolizing cytochrome P450 enzymes are targets of ??-3 fatty

acids. *J. Biol. Chem.* **285,** 32720–32733 (2010).

95. López-Vicario, C. *et al.* Inhibition of soluble epoxide hydrolase modulates inflammation and autophagy in obese adipose tissue and liver: role for omega-3 epoxides. *Proc. Natl. Acad. Sci. U. S. A.* **112,** 536–41 (2015).

96. Zhang, G. *et al.* Epoxy metabolites of docosahexaenoic acid (DHA) inhibit angiogenesis , tumor growth , and metastasis. *Pnas* **110,** 6530–6535 (2013).

97. Angelica, M. D. & Fong, Y. NIH Public Access. *October* **141,** 520–529 (2008).

98. Jung, F. *et al.* Effect of cytochrome P450-dependent epoxyeicosanoids on Ristocetin-induced thrombocyte aggregation. *Clin. Hemorheol. Microcirc.* **52,** 403–416 (2012).

99. Karishma, K. K. & Herbert, J. Dehydroepiandrosterone (DHEA) stimulates neurogenesis in the hippocampus of the rat, promotes survival of newly formed neurons and prevents corticosterone-induced suppression. *Eur. J. Neurosci.* **16,** 445–453 (2002).

100. Moriguchi, S. *et al.* Stimulation of the Sigma-1 Receptor by DHEA Enhances Synaptic Efficacy and Neurogenesis in the Hippocampal Dentate Gyrus of Olfactory Bulbectomized Mice. *PLoS One* **8,** 1–10 (2013).

101. Martineau, L. C. & Gardiner, P. F. Insight into skeletal muscle mechanotransduction: MAPK activation is quantitatively related to tension. *J. Appl. Physiol.* **91,** 693–702 (2001).

102. Hu, X. *et al.* Transgenic Overproduction of Omega-3 Polyunsaturated Fatty Acids Provides Neuroprotection and Enhances Endogenous Neurogenesis after Stroke. *Curr. Mol. Med.* **13,** 1465–1473 (2013).

103. Therapy, A. Amidst the Hype , the Neglected Potential for Serious Side Effects Aberrant Vascular Proliferation in. 115–119 (2001).

104. Crisan, M. *et al.* A Perivascular Origin for Mesenchymal Stem Cells in Multiple Human Organs. *Cell Stem Cell* **3,** 301–313 (2008).

105. Manuscript, A. Treatment of Cardiovascular Disease. **10,** 244–258 (2013).

106. Seib, F. P., Prewitz, M., Werner, C. & Bornhäuser, M. Matrix elasticity regulates the secretory profile of human bone marrow-derived multipotent mesenchymal stromal cells (MSCs). *Biochem. Biophys. Res. Commun.* **389,** 663–667 (2009).

107. Miki, Y. *et al.* The advantages of co-culture over mono cell culture in simulating in vivo environment. *J. Steroid Biochem. Mol. Biol.* **131,** 68–75 (2012).

108. Dominguez, F. *et al.* Embryologic outcome and secretome profile of implanted blastocysts obtained after coculture in human endometrial epithelial cells versus the sequential system. *Fertil. Steril.* **93,** (2010).

109. Pedersen, T. O. *et al.* Endothelial microvascular networks affect gene-expression profiles and osteogenic potential of tissue-engineered constructs. *Stem Cell Res. Ther.* **4,** 52 (2013).

110. Cells, E., Whyte, M., Ashton, P. & Genever, P. G. Regulation of Mesenchymal Stem Cell Activity. **20,** (2011).

111. Fischbach, C. *et al.* Cancer cell angiogenic capability is regulated by 3D culture and integrin engagement. *Proc. Natl. Acad. Sci. U. S. A.* **106,** 399–404 (2009).

112. Huebsch, N. *et al.* NIH Public Access. **9,** 518–526 (2010).

113. Mcfadden, B. & Heitzman-powell, L. HHS Public Access. **8,** 1699–1712 (2015).

114. Ruiz, E. J., Oeztuerk-Winder, F. & Ventura, J.-J. A paracrine network regulates the cross-talk between human lung stem cells and the stroma. *Nat. Commun.* **5,** 3175 (2014).

115. Hoeben, A. *et al.* Vascular endothelial growth factor and angiogenesis. *Pharmacol. Rev.* **56,** 549–580 (2004).

116. Abdeen, A. a, Lee, J., Mo, S. H. & Kilian, K. Spatially defined stem cell-laden hydrogel islands for directing endothelial tubulogenesis. *J. Mater. Chem. B* **3,** 7896–7898 (2015).

117. Shao, R. & Guo, X. Human microvascular endothelial cells immortalized with human telomerase catalytic protein: A model for the study of in vitro angiogenesis. *Biochem. Biophys. Res. Commun.* **321,** 788–794 (2004).

118. Gattazzo, F., Urciuolo, A. & Bonaldo, P. Extracellular matrix: A dynamic microenvironment for stem cell niche. *Biochim. Biophys. Acta - Gen. Subj.* **1840,** 2506–2519 (2014).

119. McKinnon, D. D., Domaille, D. W., Cha, J. N. & Anseth, K. S. Bis-aliphatic hydrazone-linked hydrogels form most rapidly at physiological pH: Identifying the origin of hydrogel properties with small molecule kinetic studies. *Chem. Mater.* **26,** 2382–2387 (2014).

120. Rundhaug, J. E. Matrix Metalloproteinases , Angiogenesis , and Cancer. *Clin. Cancer Res.* **9,** 551–554 (2003).

121. Omura, K. & Swern, D. Oxidation of alcohols by 'activated' dimethyl sulfoxide. a preparative, steric and mechanistic study. *Tetrahedron* **34,** 1651–1660 (1978).